An Intrinsic Relationship between Molecular Structure in Self-Assembled *n*-Alkylsiloxane Monolayers and Deposition Temperature

Atul N. Parikh† and David L. Allara*,†,‡

Department of Materials Science and Engineering and Department of Chemistry, Pennsylvania State University, University Park, Pennsylvania 16802

Issam Ben Azouz and Francis Rondelez*

Laboratoire de Physico-Chimie des Surfaces et Interfaces,§ Section de Physique et Chimie, Institut Curie, 11 Rue Pierre et Marie Curie, 75005 Paris, France

Received: January 24, 1994; In Final Form: May 3, 1994•

We have studied the effect of preparation temperature, in the range 5–65 °C, on the structures of *n*-octadecylsiloxane monolayers prepared by self-assembly from dilute solution of *n*-octadecyltrichlorosilane onto the surface of freshly hydrated, oxidized silicon substrates. Structural features of the films were characterized using a combination of liquid drop contact angle measurements, null ellipsometry, and infrared transmission spectroscopy. The contact angle data confirm a previously reported observation of a critical temperature, $T_c \sim 28 \pm 5$ °C, below which the surface energy is constant at a near-limiting value of a pure CH_3 surface and above which the surface energy monotonically increases with increasing temperature. Coverages and chain organization, as measured by ellipsometry and vibrational spectroscopic features (peak positions and integrated intensities of methylene C–H stretching modes), respectively, show changes in the same temperature region as the wetting behavior. We conclude that when prepared below T_c, the films exhibit a heterogeneous structure with closely spaced islands of densely packed, nearly *all-trans* alkyl chains arranged nearly vertical to the surface. In contrast, when prepared above T_c, the films exhibit monotonically diminishing coverage with increasing preparation temperature and the alkyl chains increasingly assume higher contents of conformational disorder. Further, the infrared data indicate that these higher temperature films are heterogeneous with coexisting domains of high and low chain conformational ordering. All the data, taken together, are in good conformity with a film formation mechanism which involves, prior to siloxy group cross-linking, the intervention of intermediate structural phases of mobile alkylsiloxy species adsorbed on a water layer adjacent to the solid substrate surface. In support of this mechanism, a strong parallel is apparent between T_c and the triple point temperature at which gas (G), liquid-expanded (LE), and liquid-condensed (LC) phases coexist for C_{18} chain Langmuir monolayers at the air/bulk water interface. Below T_c the self-assembled film structure is similar to that of the nearly pure LC Langmuir phase while above T_c the film structure is similar to that of coexisting LE and LC phases. Deviations of the self-assembled film structures for the analogous equilibrium Langmuir phase structures occur at higher preparation temperatures and are rationalized in terms of both the known occurrence of nonequilibrium phases in Langmuir films above the triple point temperature and the relative acceleration of the Si–O–Si cross-linking reaction in the self-assembled film to form structures with frozen-in defects.

1. Introduction

Preparation of tailored monomolecular surface films with molecular level control over structural order and composition represents an important goal of contemporary surface chemistry.[1] Within this framework, the study of self-assembled monolayers (SAMs) and their applications has expanded considerably in recent years, encompassing now a range of topics including wetting,[2] adhesion,[3] electrochemistry,[4] optoelectronic and molecular electronic devices,[5] nanotechnological structures,[6] bioactive surfaces,[7] and, in general, fundamental studies of quasi-two-dimensional systems. One of the most widely used classes of SAMs is based on organosiloxanes,[8] and continuing interest has been focused on the highly hydrophobic and oleophobic films derived from *n*-alkyltrichlorosilanes ($RSiCl_3$). Through a combined process of adsorption and hydrolysis, dilute solutions of these trichlorosilane molecules in organic solvents can lead to spontaneously assembled, often highly organized, alkylsiloxane ($RSiO_x(OH)_y$) monolayer films at the surfaces of many solids, most notably oxides (SiO_2, Al_2O_3, SnO_2, silicate glasses, TiO_2, etc.). There has been a popular focus on the self-assembly of films of the octadecyl derivative (termed OTS for formation from octadecyltrichlorosilane) onto oxidized, planar silicon substrates (SiO_2/Si),[9] and the general state of knowledge about *n*-alkylsiloxane films is almost always extrapolated from OTS/SiO_2/Si studies.[1b,5] This continuing interest has several bases. First, these films can be prepared with a value of the critical surface tension which approaches what is regarded as the limiting, minimal value for a pure, close-packed CH_3 surface.[10] Second, these films are remarkably stable to both thermal treatment[11] and chemical attack.[12] Third, these films can be deposited on a variety of substrates, a strong contrast to other popular self-assembled monolayer systems such as *n*-alkanethiolates on gold[1b,2b,c,13] which are substrate specific. While these attributes continue to provide considerable opportunities for applications to surface property modification, as well as the understanding of monolayer structures and wetting properties, an incomplete understanding of the mechanism of film formation exists as manifested in the variety of procedures used to prepare supposedly similar films and the significant lab-to-lab discrepancies in the reported film structures. With regard to the latter, a variety of characterization techniques have been used to probe these

† Department of Materials Science and Engineering.
‡ Department of Chemistry.
§ Laboratoire associé au C.N.R.S. (URA 1379) et à l'Université de Paris VI.
• Abstract published in *Advance ACS Abstracts*, July 1, 1994.

0022-3654/94/2098-7577$04.50/0

monolayer structures, including contact angle measurements,[10,14] infrared attenuated total reflection spectroscopy (IR-ATR),[14] X-ray photoelectron spectroscopy (XPS),[10a] infrared–visible sum-frequency generation,[15] ellipsometry,[14,16] X-ray reflectivity (XRR),[16] grazing incidence X-ray diffraction (GIXD),[17] and atomic force microscopy (AFM).[18] In spite of this extensive work, important details of the structures of limiting high quality films remain uncertain. For example, whereas IR studies[14b,e] support a structure with the alkyl chains in predominantly *all-trans* conformations and with the chain axes tilted on average at an angle in the range 5°–15° from the surface normal, a structural state consistent with a uniform crystalline-like phase, in contrast, GIXD studies[17] support very short translational ordering correlation lengths of ~45 Å which suggest significant disordering is present. Similarly, for incomplete adsorption films, Angst and Simmons[19] using IR-ATR spectroscopy and Wasserman et al. using XRR[16] have suggested the formation of homogeneously disordered, uniform films, while Tidswell et al.[17] using GIXD measurements and more recently Schwartz et al.[18b] and Barrat et al.[18a] using AFM confirm the original results of Sagiv[11a] and Garoff[20] which indicate islandlike, heterogeneously disordered films. One obvious possibility for such discrepancies is that significant lab-to-lab variabilities exist in the synthetic procedures. Clearly, the identification of the key controlling synthesis parameters and the development of detailed relationships between these and the structural properties of the resulting monolayers are urgently needed in order to provide advances in our understanding and applicability of this important class of self-assembled monolayers.

Quite recently, reports have appeared in which two experimental variables have been identified to be of crucial importance during preparation, namely, the solution temperature[10c,d] and the presence of interfacial water.[21] These two are linked together via a recently proposed mechanism[10d,22] which requires a temporary presence on the substrate of an ultrathin, interfacial water film. In this mechanism, the water layer allows the formation of a highly organized, transient Langmuir-type film of hydrolyzed OTS molecules which subsequently forms the final polymerized film by compliant cross-linking of the siloxy network. Since the proposed mechanism offers the promise of a rational way to design synthetic procedures to produce desired film structures, it is critical to establish its validity. In previous reports,[10c,d] wetting measurements were used to establish the role of preparation temperature over a wide range of temperature (5–60 °C) for a series of *n*-alkyltrichlorosilane monolayers. However, no structural characterization was performed, and so the most critical questions of the structural effects remained unanswered. It was observed in these studies that monolayers with low wettabilities (critical surface tension, γ_c) comparable to those of close-packed CH_3 surfaces[10,28] are obtained below an upper threshold temperature, T_c. On the other hand, above T_c, the critical surface tension values were observed to deteriorate quickly with increasing temperature, an effect consistent with formation of *disordered* surfaces with diminished fractions of exposed CH_3 groups and increasing exposure of more wettable CH_2 or surface silanol groups.[23] Since T_c was observed to be dependent directly on the chain length of the assembling molecules and independent of the solvent used in the adsorption process, it was further proposed that T_c is an intrinsic property of the monolayer system, a property exhibiting a strong parallel with the temperature-dependent phase behavior of Langmuir surfactant films.[24] On this basis, it is predicted that each chain-length film prepared below the corresponding T_c should exhibit maximal packing density and organization relative to those films made above T_c and that above T_c the structural ordering should increasingly decay with increasing temperature. With these predictions in mind, the present study was designed to systematically correlate film structure as a function of preparation temperature. In order to concentrate on the characterization efforts, the octadecyl derivative was singled out for careful study. This choice was based on the observation[10c,d,22] that T_c for OTS occurs conveniently at near ambient temperature and also on the fact that it is the most commonly studied alkylsiloxane film[1b] and thus of significant specific interest compared to other chain lengths. Our results with these OTS films conclusively confirm the existence of a critical deposition temperature and show that significant differences in film structure exist above and below this temperature. Further, these differences are completely consistent with a Langmuir-type mechanism for self-assembly. A benefit of this work is the identification of a means of preparing maximally organized samples which can provide a common ground for comparison of characterization experiments from different laboratories.

2. Experimental Section

The experimental approach consisted of the preparation of monolayers of OTS onto clean surfaces of oxided (native) silicon over a range of precisely controlled temperatures (±0.5 °C) between 5 and 65 °C according to the procedures proposed by Brzoska and co-workers[10c] and the subsequent analyses of the films by sessile drop contact angle measurements, single-wavelength null ellipsometry, and transmission infrared spectroscopy (TIRS).

2.1. Materials. Octadecyltrichlorosilane of 95% purity (Petrarch Systems, Bristol, PA) was distilled at reduced atmosphere (10^{-2} kPa) immediately prior to use and collected in clean, dry glass vials which were capped off with a septum. Aliquots were withdrawn by a dry syringe as needed. Hexadecane (Gold Label; Aldrich Chemical, St. Paul, MN) was dried by extraction over sulfuric acid (Baker Analyzed Grade, J. T. Baker, Philipsburg, NJ) and dehydrated over active alumina (grade II) just prior to use. All other *n*-alkanes were obtained from Aldrich with the manufacturer's listed purity of at least 99% (water concentration <0.001 M) and used directly for wetting measurements. Chloroform and carbon tetrachloride were of reagent grade (Aldrich). Organic-free, deionized water of high resistivity (>18.0 mΩ/cm) was obtained by processing water through a Millipore Purification System (Bedford, MA) consisting of a reverse osmosis deionization cartridge and an ion exchange/carbon purification system. The silicon substrates were obtained from Harrick Scientific (Ossining, NY) as square plates with either 2.5- or 3.8-cm sides. Both sides were finished to a high polish, and one side was wedged slightly off-parallel from the other in order to minimize interference fringes in TIRS measurements.

2.2. Sample Preparation. The octadecylsiloxane films were prepared[10] by reacting freshly cleaned, oxided (native) silicon wafers with 2.5 mM solutions of OTS in a mixed hexadecane/CCl_4 70:30 solvent for 60 min. In order to check the effect of longer immersion times, two additional experiments were conducted using 12-h immersion for samples prepared at 20 and 53 °C. The reaction solutions were maintained at a constant temperature (±0.5 °C) in an argon-purged glovebox and the sample introduction and withdrawal were carried out under this atmosphere. The silicon substrates were first cleaned by stripping of any organic contaminants using a combination of chemical and photochemical methods.[25] Initially, the silicon samples were ultrasonically degreased in chloroform, and each side of the degreased substrates was then oxidized for 30 min in a UV/ozone[26] cleaner (Model uvc-100, Boekle Industries, Philadelphia, PA). This was followed by immersing the samples in peroxysulfuric acid solution (4:1 v/v mixture of H_2SO_4 and 30% H_2O_2 at 110 °C) (*caution: this mixture reacts violently with organic materials and must be handled with extreme care*) for approximately 10–15 min. These cleaned substrates were washed thoroughly in purified water several times and dried at 100 °C for a short time. The final cleaning involved UV/ozone treatment of each side for 30 min. The silanization reactions were carried out in glass containers at the selected temperatures. All the reaction vessels used were thoroughly precleaned using chromic/

sulfuric acid solutions followed by extensive washing with deionized, low organic water and finally air-dried in an oven. After removal from the reaction solution, the film-covered wafers were washed extensively with chloroform under ultrasonic conditions to remove all excess reactants.

2.3. Contact Angle Measurements. The oleophobic wettability characteristics of the samples were measured using a laser-assisted, tilt stage technique for simultaneous measurements of advancing and receding contact angles.[27] In this method, a collimated beam of He–Ne laser light is allowed to irradiate the sessile drop along the normal to the substrate surface. The drop behaves like a convex mirror and diverges the beam at all finite angles. The divergence of the beam for contact angles below 45° is proportional to the contact angle at the triple contact line. The reflected beam is then collected over a flat surface at a known height perpendicular to the incident beam. The diameter of the reflection then can be translated into the static contact angle of the drop using a simple trigonometric relationship. In order to determine advancing and receding contact angles simultaneously, the substrate stage is slowly tilted until the drop begins to move by gravity. Under these conditions, the reflection image is distorted away from its static circular boundary along the tilt axis. The radii of curvatures along the slip axes then can be translated into advancing and receding contact angles. The contact angles, both advancing and receding, for the homologous series of liquid n-alkanes, octane, decane, dodecane, tetradecane, and hexadecane were carefully measured at three different spots for each silanized surface. The errors in these measurements were ±0.5° for contact angles below 45°. All experiments were conducted in a dark room under ambient atmosphere. The advancing contact angles then were used to derive the critical surface tension (γ_c) values of the monolayers using the Zisman method.[28]

Water contact angles were measured using a standard goniometric apparatus (Ramé-Hart Model 100). Static, sessile drops (10–30 μL) were delivered from a flat-tipped micropipet, and the measurements were done under saturated water vapor in a controlled atmosphere chamber; however, no difference between ambient and saturated vapor measurements was detected within experimental error. The reported values are averages of three different drops on each sample surface. Spot-to-spot variation on a given sample was less than ±1°, and the overall accuracy in the measurements was less than ±3°.

2.4. Optical Ellipsometry. *2.4.1. Measurements.* A null ellipsometer (Rudolph Model AutoEl II, Rudolph Research, Fairfield, NJ) operating at 632.8 nm and at a 70° angle of incidence was used with a beam spot of 2 mm. Measurements were made at five different spots on each sample. The phase shift and amplitude ratio ellipsometric parameters,[29] Δ and Ψ, respectively, were determined directly from the observed polarizer and analyzer angles. The instrumental precision of the ellipsometric angles was 0.04°, and the overall, sample-to-sample errors in terms of final calculated OTS film thicknesses, as detailed below, are within ±1 Å. The time of a single measurement was approximately 1 min, and the complete set of multiple measurements for each bare substrate was completed within 10 min after precleaning. This time was minimized in order to reduce the chances of adventitious contaminant adsorption. The ellipsometry readings for several (up to three) predeposition cleaning cycles were always found identical within experimental error. The ellipsometric parameters were recorded for all the samples during an independent cleaning cycle and were not measured during the final predeposition cycle. After silanization the wafers were found to be considerably resistant to tenacious contamination. For example, reproducible ellipsometry and wetting data were obtained even after several months air exposure in a sealed storage container, provided only that the wafers were ultrasonicated in chloroform prior to the measurements.

2.4.2. Film Thickness Calculations. Film thicknesses were determined from the ellipsometric parameters using standard classical electromagnetic theory[29] in conjunction with a parallel-layer model consisting of an air/film/substrate structure. The treatment assumes that the total sample consists of semiinfinite, parallel slabs, each a uniform material of homogeneous composition described by a single optical (or, alternatively, dielectric) function, assumptions which are quite valid for our samples. Independently determined values of the substrate optical functions were assigned (see below) for the thickness calculations. With the current level of precision of the single-wavelength measurements, the ellipsometry equations do not allow an independent determination of both the optical function and the thickness of the OTS film from the Δ and Ψ values. Therefore, the film thickness was determined using independently assigned values of the substrate and film optical (or, alternatively, dielectric) functions. The amorphous oxide and crystalline silicon phases, as well as any adsorbed water phase, associated with the substrate are treated as optically isotropic and thus assigned scalar optical (or dielectric) functions. In contrast, as will be discussed below, since the OTS film consists of oriented alkyl chains, it should be considered as an optically anisotropic medium for which the optical function is described by a second rank tensor. Further, since the OTS film exhibits no optical absorption at 632.8 nm, the optical function is a real quantity. The actual calculations were performed using algorithms based on matrix formulations of the appropriate electromagnetic equations, and details can be found elsewhere.[16,30,31]

The independent assignment of the correct sbustrate optical functions for the OTS/substrate structure is most conveniently done by an independent ellipsometric analysis of the exact same substrate structure but without an OTS film overlayer, i.e., a "bare" substrate. A close experimental approximation is provided by the measurement of the initial freshly cleaned, hydrated, oxided silicon sample specifically used in the OTS film preparation of interest. The substrate in this case is a three-phase structure consisting of an ultrathin water layer[19,32] estimated to be of monolayer quantity,[32b] a native oxide layer of ~1.5–2-nm thickness, and the pure Si substrate.[33] Using these reference substrates, rigorous calculations of final OTS film thicknesses follow by explicitly specifying for each separate substrate the exact thicknesses and dielectric functions for each layer in the substrate structure. While the use of this substrate approximation is experimentally convenient in terms of sample preparation procedures, there are two specific problems to address in the final thickness calculations. First, the specification of exact SiO_2 and H_2O layer thicknesses requires additional characterization beyond the present single-wavelength ellipsometry measurements, an inconvenient procedure for analysis of a large number of samples. Second, the bare substrate structure is not expected to be identical to that in the OTS/substrate structure since the thickness of the initially adsorbed ultrathin water film will not necessarily remain the same after the deposition of the OTS film, and any change will lead to errors in the calculated OTS thickness of a size approximately that of the change in the water layer thickness. Each of these points is discussed in turn below.

In order to circumvent the first problem above, the substrate was approximated as a pseudo-one-phase structure with an optical response described by a single (complex scalar) dielectric constant. On this basis, a pseudodielectric function was determined for the bare substrate from the measured ellipsometric response using an air/substrate model for the calculations. In turn, this pseudodielectric function was used for the OTS thickness calculation from the final ellipsometric measurements using an air/film/substrate model. The errors in this approximation,[34] relative to a rigorous consideration of all the constituent layers, are substantially less than the sample-to-sample experimental error (see above).

Quantitative measurements of any changes in the adsorbed water layer between bare substrate and OTS/substrate structures were not made in this study, but it is clear from the ±1-Å sample-to-sample reproducibility in repeat preparations that any changes in the water layer thicknesses are constant within this range.

However, estimates of the actual magnitude of expected changes can be made from literature reports. It has been reported by Scott and Traiman[32b] that the surface of a high surface area silica gel, equilibrated at 23 °C in 50% relative humidity, possesses approximately three monolayers of adsorbed water. However, since the cleaned SiO_2/Si surfaces used for our OTS monolayer preparation are actually mildly heated (<100 °C) briefly just before immersion, the water coverage is estimated to be at least one monolayer but clearly less than three. Angst and Simmons[19] have reported infrared spectroscopic results which show that, for the case of fully hydrated, oxidized silicon surfaces, the amount of adsorbed water is slightly higher after OTS film formation. Assuming that the water structure at the SiO_2 surface is not perturbed upon silanization, we estimate from the integrated areas of Angst and Simmons' reported O–H stretching spectra than an $\sim^1/_3$ increase in the amount of adsorbed water results upon OTS film formation. On this basis and using a maximum estimate of two monolayers for the initial water film, the maximum increase in an equivalent water layer thickness would be $^2/_3$ of a monolayer or ~1.7 Å upon silanization for a monolayer thickness of ~2.5 Å.[35] In terms of the OTS film thickness calculation procedure, our reported thicknesses accordingly would be overestimated by ~1.3 Å, for this maximum adsorption case, since the ellipsometric response of any adsorbed water in excess of that initially present on the bare substrate would be counted in the film thickness calculation as a contribution from the OTS film phase. While we caution that this estimate is approximate, since the exact nature of SiO_2 surfaces, the ambient exposure times, and the water vapor partial pressures are expected to be different for all the above data, the estimate does set a useful lower limit on the range of thickness values derived from the ellipsometric measurements on these films.

In the calculation of the OTS film thicknesses, the optical response of OTS layer can be treated with two limiting models: (1) *isotropic*, with the refractive index described by a scalar quantity, n_{iso}, and (2) *anisotropic*, with the optical function defined as a second rank, refractive index tensor with uniaxial symmetry and elements based on principal refractive index values, $n_\parallel$ and $n_\perp$, parallel and perpendicular to the alkyl chain axis, respectively. For cases of high-coverage, high-density films for which the chains are fully extended (see section 3.3), the second model is clearly more appropriate than the first, but for lower coverage films, in which the chains become increasingly conformationally disordered (see section 3.3), the decay of a unique chain director (C–C–C backbone axis) approaches the limit for which the isotropic model is valid. Since it was observed (section 3.3) that the conformational order of the OTS films varies over the range of films studied, it was not possible to calculate rigorously correct film thicknesses using any single-film model so both were used in order to set limits. For these calculations it was first necessary to select a self-consistent set of the values of the optical functions at 632.8 nm, the wavelength of the present study. Previous studies have utilized values of n_{iso} in the range 1.45[16] to 1.50.[1b] The latter value is quite reasonable for a high-density hydrocarbon film since it is within the range of values reported for polyethylene, 1.49–1.53.[36] Previous studies of oriented Langmuir films of octadecanoic acid offer values of 1.484 and 1.559 for $n_\parallel$ and $n_\perp$, respectively.[37,38] For a medium composed of randomly oriented linear chains and thus exhibiting an isotropic response, the above values of $n_\parallel$ and $n_\perp$ collapse to an average value of $n_{iso} = 1.509$-$[^1/_3(2n_\parallel + n_\perp)]$, a value within the range of those above for polyethylene-like media. On this basis, the OTS film thicknesses were calculated using $n_{iso} = 1.50$ and the above values of $n_\parallel$ and $n_\perp$. The details of the calculations in the isotropic approximation have been reported previously.[39] The anisotropic medium thickness calculations are based on a 4 × 4 matrix method, and details can be found elsewhere.[30,31] The optical function tensor for the anisotropic calculation was constructed on the basis of chains oriented at an angle of ~11° from the surface normal (see section 3.3 on TIRS determination of tilt angles). One should note that both the isotropic and anisotropic calculations are based on constant refractive index values, a condition which corresponds to a constant uniform density model of the OTS film for which any changes in the ellipsometric parameters are interpreted as changes in film thickness, not film density. For the cases of partial monolayers, where looser packing and higher *gauche* conformer content exist (section 3.3), lower densities tending toward (but not reaching) those of a liquid state would be appropriate, and a decrease in the values of the refractive index from 1.50 would be expected. We have considered these effects in the isotropic approximation, and our calculations show that the use of a value of $n_{iso} = 1.50$ would lead to a maximum underestimation of the film thicknesses by ~0.8 Å for the most extreme case of a completely liquidlike film.[40]

Since it is convenient to discuss the structures of the films in terms of changes in the surface coverage of chains, a useful relative measure of the coverage was calculated from the relationship $f_e = d_e/d_t$, where d_e is the ellipsometrically derived thickness and d_t is the maximum thickness which would be obtained for a perfectly packed, densest assembly of ideal rigid-rod-like alkyl chains standing vertically to the surface. The value of d_t is assigned as 26.2 Å, the length of an *all-trans* octadecylsiloxy chain.[16] A limiting value of $f_e = 1$ would correspond to an OTS film with a near-theoretical maximum surface density of chains, essentially equivlaent to that of crystalline polyethylene in the *a,b* plane. Lower values indicate incomplete coverages with reference to this ideal state. All values of coverages given in this paper are based on the above equation.

2.5. Transmission Infrared Spectroscopy. Infrared transmission spectra were collected using a Fourier transform spectrometer (Bomem Model MB-100, Québec, Canada) operating at 2-cm^{-1} resolution with an unpolarized beam striking the sample at normal incidence. The beam diameter was controlled at 6 mm by an aperture placed adjacent to the sample. The resulting interferograms from multiple, coadded, scans were Fourier transformed with triangular apodization and zero-filling to increase the point density by a factor of 16, which yields an effective resolution of less than 0.2 cm^{-1}. Such interpolations do not involve smoothing of the data points and thus allow accurate determination of peak positions.[41] The spectra of silanized films were referenced against the spectra obtained for the same clean, bare substrate wafers before silanization. Minor differences in alignment between the sample and reference runs often led to troublesome artifacts in the spectral base lines. In order to minimize these problems, a sacrificial protocol was developed which involved first collecting the spectrum of a silanized sample and then immediately oxidizing the film away using a UV–ozone treatment during which the sample mounting in the spectrometer remained completely undisturbed. This process was carried out by mounting UV (184 nm) lamps immediately adjacent to the sample faces in the spectrometer compartment and purging very slowly with dry air which provided oxygen for ozone generation. In this way, two sets of reference spectra were available for each sample, and the most artifact-free ratio spectra were selected from the pairs. All spectra are reported in the transmission absorbance units, $-\log(T/T_0)$, where T and T_0 are the emission power spectra of each sample and reference, respectively.

For selected samples prepared at low silanization temperatures, temperature-dependent spectra were generated at intervals of 20.0 °C over a range of sample temperatures between 25 and 190 °C with the substrate temperature held constant to within ±0.5 °C. In order to prevent oxidative degradation of the sample, the spectrometer was purged with nitrogen. Absorption spectra were calculated using a reference spectrum collected at room temperature, as described above.

3. Results

3.1. Wetting. The plot of critical surface tension (γ_c) as a function of silanization temperature, displayed in Figure 1, clearly

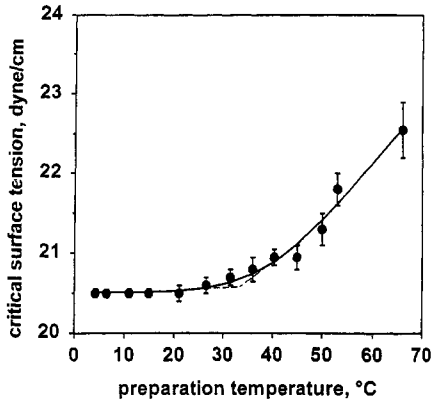

Figure 1. Preparation temperature dependence of critical surface tensions of OTS monolayers on SiO_2/Si surfaces. The solid lines are obtained by curve-fitting a sigmoidal function (see text for details).

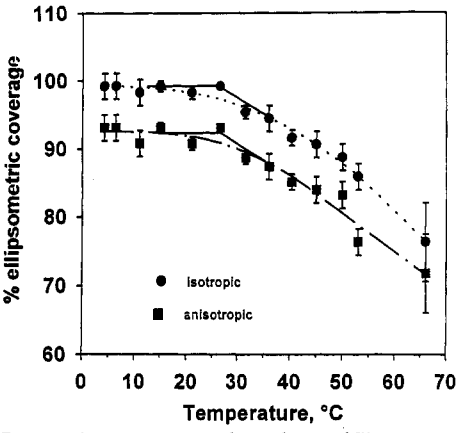

Figure 2. Preparation temperature dependence of film coverages of OTS monolayers on SiO_2/Si substrates. The coverages are derived from ellipsometric film thicknesses values normalized to a maximum value of 26.2 Å, the selected length of an extended *all-trans* octadecylsiloxy moiety. The solid lines are obtained by a curve-fitting a sigmoidal function. The two curves represent the results of the use of two limiting models, isotropic and anisotropic, for the thickness calculations (see text for details).

reveals two distinct regimes: a low-temperature plateau of constant γ_c and a high-temperature region where γ_c is increasing monotonically. The crossover between these two regimes can be characterized by a well-defined temperature, denoted as T_{cw}, which was assigned a value of 34.0 ± 3 °C by fitting the data with a standard sigmoidal function[42] and selecting the intersection point of the tangents drawn from the variable and plateau regions. Below T_{cw} the critical surface tensions of the silanized samples all were 20.5 ± 0.5 mN m^{-1}. This latter value is generally accepted as an indication of a densest-packed methyl surface.[10] The higher values observed above T_{cw} indicate formation of a mixed surface consisting of backbone methylene and terminal methyl groups,[28,43] consistent with formation of loosely packed, disorganized assemblies of alkyl chains. The results of these measurements are in excellent conformity with those obtained by Brzoska et al.,[10c] in terms of both the trends and the actual values obtained for γ_c.

The hysteresis in the contact angle measurements was determined from the quantity $\delta = \cos(\theta_a) - \cos(\theta_r)$, where θ_a and θ_r are advancing and receding contact angles, respectively. The average value of δ for all probe liquids on the silanized wafers was observed to have a temperature-independent value of 0.025 ± 0.01. These observations are in good conformity with those obtained previously by Brzoska et al.[10d,22] Similar measurements have been made by Barrat and co-workers,[10b] using a different preparative strategy, and our data are in qualitative agreement with theirs (ref 10b). However, these authors suggest that, at high preparation temperatures, higher values of hysteresis can be observed, which we do not observe here. While macroscopic theories exist to explain contact angle hysteresis,[37] molecular descriptions of the origins are yet to be fully defined[44] and workable models for quantitative interpretation of wetting hysteresis data in microscopic terms are not available, to our knowledge. However, phenomenological models[45] suggest that the hysteresis in contact angle values is due to the presence of chemical or physical heterogeneities and/or slow surface reorganization[46] (surface dynamics). On this basis, some qualitative inferences can be made. Below T_{cw}, the low hysteresis values observed are consistent with the formation of densely-packed monolayers with a uniform surface of pure methyl character. Above T_{cw}, where formation of disorganized monolayers is observed, the low hysteresis values imply stable structures in which the domain sizes do not exceed ~0.1 μm.[47]

For samples prepared below T_{cw}, water contact angles were measured and found to be 114 ± 2°, in good agreement with those reported for close-packed methyl surfaces.[2c,d]

Experiments at extended immersion times of 12 h (versus 1 h) were conducted on two sets of samples prepared at 20 and at 53 °C, spanning T_{cw}. The observed values of γ_c are 20.4 ± 0.2 and 21.0 ± 0.3 mN m^{-2}, respectively, while for the 1-h preparation times the values (see above) are 20.4 ± 0.2 and 21.8 ± 0.2 mN m^{-2}. These observations show, contrary to what might be expected, that film formation at the higher temperatures occurs more slowly and does not appear to lead to low γ_c values, even at long reaction times.

3.2. Ellipsometry. In Figure 2, the fractional monolayer coverages calculated from the ellipsometric thicknesses are plotted as functions of silanization temperatures. We point out that because of the uncertainty of the changes in adsorbed water upon OTS film formation the absolute values of these coverages should be considered as estimates (see section 2.4), but we do emphasize that the relative trends are quite meaningful. Two curves are shown, each representing the thickness calculation carried out on the basis of a specific ideal limiting structure of the OTS film. In one case, labeled anisotropic, the film is considered to consist of a uniform, densest-packed ensemble of *all-trans* conformation alkyl chains oriented vertically to the substrate surface (the crystalline rigid rod limit). Since the optical response of the film in this limit is directionally dependent, the thickness calculations require this anisotropy to be explicitly considered in terms of a refractive index tensor (see section 2.4). In the isotropic case, the film is considered as an ensemble of completely conformationally disordered chains (the liquid state limit) with no directional dependence of the optical response and thus appropriately described by a scalar refractive index (see section 2.4). Both curves clearly demonstrate a dependence of the underlying ellipsometry data on the preparation temperature as defined by the presence of two well-defined regimes, a low-temperature, constant-coverage regime and a high-temperature regime in which the surface coverage is monotonically declining. The onset of the declining coverage regime is marked by a characteristic temperature (calculated from a sigmoidal fit as for the wetting data in section 3.1), denoted as T_{ce}, with a value equal to 26 ± 3 °C. Finally, with regard to the absolute coverages shown in Figure 2, we remark that our best estimate of the changes in adsorbed water (see section 2.4) indicates that the coverages could be offset to lower values by as much as ~7% (~1.5 Å in thickness).

The films prepared below T_{ce} exhibit the maximum coverage, as well as the lowest surface energy (section 3.1), observed in these experiments and can be considered as having structures much closer to the ideal rigid-rod crystalline limit than the disordered, liquidlike limit. (Further support is given by the TIRS data in section 3.3.) On this basis the anisotropic model coverage value of 93 ± 4% is to be considered as more appropriate for analysis in this high-coverage regime. If consideration were made of the estimated effects of changes in the adsorbed water upon OTS deposition, as discussed above (section 2.4), the actual coverage could drop to 86%. The most extensive studies of

ellipsometric thicknesses of alkylsiloxane films are those of Wasserman et al.,[10a] who report a range of values between 22.6 and 27.6 Å for high-coverage OTS films prepared on oxidized silicon wafers. However, these values were derived using an isotropic model calculation with a scalar refractive index value of 1.45, so must be compared to our data on this basis. Normalized to the ideal limiting thickness value of 26.2 Å, the range of their thicknesses, when corrected for a refractive index value of 1.50, represents a 82–101% coverage, a range encompassing our isotropic model value of 98 ± 4% (shown in Figure 2).[48] For comparisons with other monolayer systems (see later), it is convenient to translate the above fractional coverages into absolute counts of adsorbate molecules per unit surface area (or average area per molecule) values. Since the limit of 100% coverage was selected to represent an ideal reference structure with a chain surface density of 5.42 chains nm^{-2}, equivalent to that of crystalline polyethylene in the *a,b* plane[49] (see section 2.4), the above average coverage of 93 ± 4% taken from Figure 2 would accordingly correspond to 5.04 ± 0.2 chains nm^{-2} or an average area per molecule of ~19.8 ± 0.8 Å^2. We suggest that this absolute coverage value should be regarded most reasonably as an upper limit, based on the estimated change in the coverage of adsorbed water upon film deposition (see above and section 2.4); thus, this average area per molecule should be regarded as a lower limit. In the other limit, derived from the assumption of no change in water coverage (see above), the lower film coverage value of 86% corresponds to 21.5 Å^2 molecule^{-1}. This range of 19.8–21.5 (±0.8) Å^2 is in general agreement with the values of 20.2 ± 0.2 Å^2 obtained from GIXD measurements[17] and is within experimental error of the value of 22.5 ± 2.5 Å^2 obtained from XRR measurements.[16] Averaging all these different values gives a value of ~20.7 Å^2 molecule^{-1} or a average coverage of ~89%.

Above T_{ce} the film coverage decreases almost linearly with temperature. Since the TIRS data (see following section) indicate that the alkyl chains become increasingly conformationally disordered, the use of the anisotropic calculation of film thicknesses becomes less realistic. However, in this range of intermediate disorder the isotropic limit (liquidlike) is not reached. Thus, the appropriate coverages in Figure 2 actually fall somewhere between the two curves. At 65 °C, the highest preparation temperature used, the film coverage decreases to ~75% of the maximum value, using the isotropic thickness calculation, a clear demonstration of the strong influence of the preparation temperature on the monolayer coverage. The *average* molecular areas for the set of above T_{ce} films monotonically increases from 20.5 to 24.2 Å^2 molecule^{-1} (isotropic values) with increasing temperature. These data suggest that the degree of chain organization decreases with increasing temperature.

3.3. Infrared Spectroscopy. Figure 3 displays TIRS spectra in the C–H stretching mode frequency region as functions of silanization temperature for four selected temperatures. Each spectrum is characterized by the presence of three distinct peaks in the ranges 2850–2853, 2917–2922, and 2956–2962 cm^{-1} which can be assigned straightforwardly[50-52] as primary contributions from the methylene C–H symmetric (d^+) and antisymmetric (d^-) stretching modes and the methyl C–H antisymmetric stretching modes, respectively. A careful examination of the spectra of films prepared at different temperatures shows that peak positions, line widths, and integrated peak intensities all undergo noticeable changes.

The most discernible changes occur in the frequency positions of the d^+ and d^- modes, and these data are displayed in Figure 4. Both plots show a plateau at low temperatures followed by a linearly increasing regime at higher temperatures. The onsets of the high-temperature regimes are marked by characteristic temperatures, (calculated as before) T_{cd^+} and T_{cd^-}, with values of 23 ± 4 and 24 ± 4 °C, respectively. The peak frequencies of the d^+ and d^- modes of alkyl chains are typically reported to be in the ranges 2846–2850 and 2915–2920 cm^{-1} for *all-trans* extended chains[51] and ~2856 and 2928 cm^{-1} for highly conformationally disordered chains,[52] respectively. Comparison of these values with the respective values of 2848.8 ± 0.2 and 2916.8 ± 0.2 cm^{-1} observed for the low-temperature preparation films (Figure 4) strongly infers that the OTS monolayers prepared at low temperatures are dominantly populated by *all-trans* extended chains, a structural state associated with dense packing. More pointed comparisons of the observed frequencies are possible using recently reported data on Langmuir films of relaxed heneicosanol ($C_{21}H_{43}OH$) monolayers by Buontempo et al.[53] in which the liquid-condensed (LC) phase with coverages between 4.55 and 5.0 chains nm^{-2} (22 and 20 Å^2 molecule^{-1}) exhibits d^+ and d^- frequencies in the ranges 2849.2–2849.6 and 2917.1–2917.5 cm^{-1}, respectively, in reflection spectra.[53] These peak positions correspond well with those observed in our below T_c films, and the ranges of coverages overlap with those estimated from our ellipsometry data (section 3.2). Further, complementary molecular dynamics simulations

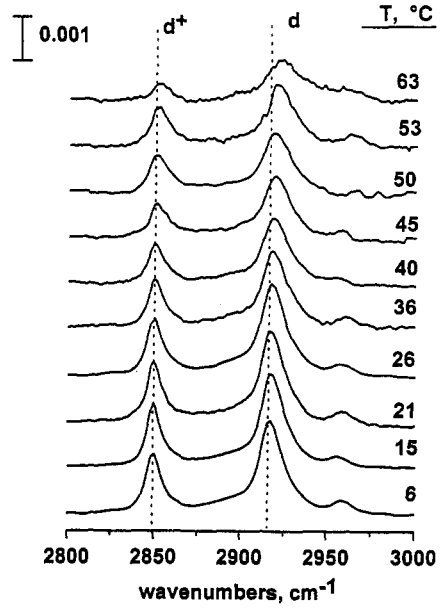

Figure 3. Transmission infrared spectra in the C–H stretching region of OTS monolayers on SiO_2/Si substrates prepared at various preparation temperatures. The intensities are given in transmission absorbance units, $-\log(T/T_0)$ where T and T_0 are the transmittivities of the SiO_2/Si substrates with and without OTS monolayers, respectively. The dashed lines are provided as a guide to the eye.

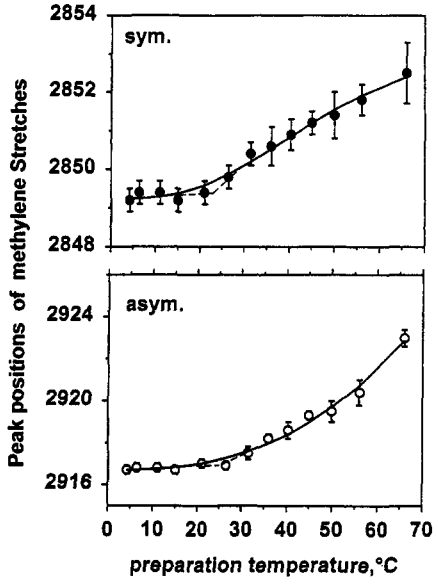

Figure 4. Positions of the peak maxima in cm^{-1} assigned to the methylene C–H symmetric (d^+) and antisymmetric modes (d^-) for OTS monolayers on SiO_2/Si substrates as a function of the preparation temperature. The solid lines are obtained by curve-fitting a sigmoidal function (see text for details).

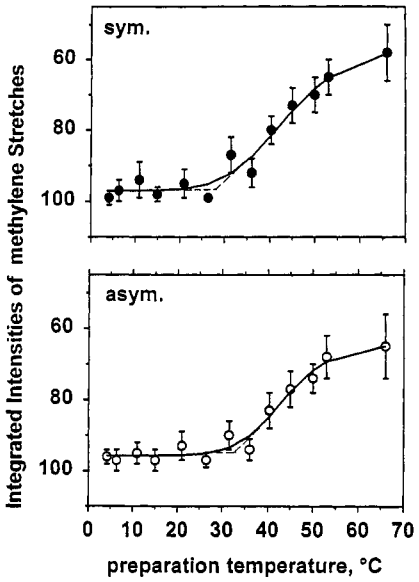

Figure 5. Intensities of the peak maxima in absorption units (as defined for Figure 3) of the methylene C–H symmetric (d^+) and antisymmetric modes (d^-) as a function of the preparation temperature. The solid lines are obtained by curve-fitting a sigmoidal function (see text for details).

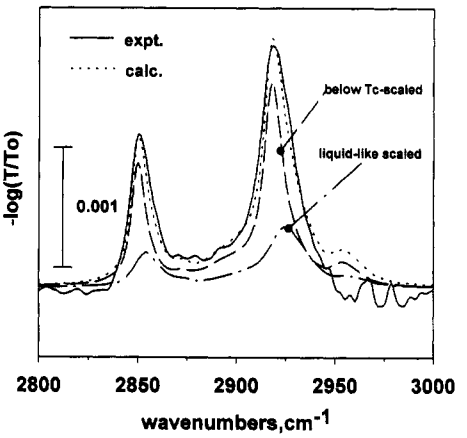

Figure 6. An illustration of a infrared line shape curve fitting for an OTS film prepared at 40 °C. The figure shows an actual infrared spectrum (solid line) of a film prepared at 40 °C and an overlay trace (dotted line) calculated using a 3:1 weighting of a below-T_c film spectrum and a simulated liquid-phase spectrum, respectively. The latter spectrum was derived using liquid-state optical properties of octadecylsiloxy molecules (for details, see text).

reported for the heneicosanol Langmuir films in the same study by Buontempo et al.[53] show that in the coverage range 18.0–22.0 Å^2 molecule^{-1}, a range which spans our ellipsometric estimates (19.8–21.5 Å^2/molecule), the above frequency range corresponds to a structural phase in which the alkyl chains possess between 96% and >99% population of *trans* conformers. Identical results have been reached by Karaborni[54] in an independent molecular dynamics study of the dense LC or solid (S) phases of Langmuir films of molecules consisting of a 19-pseudoatom alkyl chain and a carboxylate-like pseudoatom for the headgroup ($C_{19}H_{39}CO_2^-$). On the basis of the relative insensitivity of the d^+ and d^- frequencies to surface coverage, Buontempo et al.[53] have inferred that their *n*-alkanol Langmuir films contain heterogeneously assembled islands of close-packed, ordered chains. This conclusion is consistent with parallel GIXD data[55] and molecular dynamics simulations.[56] The strong correspondence of our d^+ and d^- mode frequencies with those of the Langmuir film spectra of Buontempo et al.[53] suggests the possibility of island formation in our low-temperature OTS films. This point will be discussed in more detail below. In comparison to the spectra of the low-temperature films, higher peak frequencies of the d^+ and d^- modes are observed for OTS monolayers prepared above $T_{cd^\pm}$ (Figure 4). These data suggest that significantly higher average populations of *gauche* conformers are present than for the below T_c films. The spectra apparently characterize a phase state which corresponds to neither pure crystalline nor pure liquid phases. Recent molecular dynamics simulations[54] (see above) also show that at coverages between 20.5 and 24.2 Å^2/molecule, corresponding to those estimated for our above-T_c films, the average population of *trans* segments is reduced to between 88% and 96%, a trend consistent with our observations of an increase in the $d^\pm$ peak frequencies. However, we note that the peak frequencies of our above-T_c films (~2850–2854 and ~2917–2923 cm^{-1}) are significantly higher than those reported for IR spectra of the *n*-alkanol Langmuir films (2849.2–2849.8 and 2916.5–1917.7 cm^{-1}) for which the simulations were intended so our films appear more conformationally disordered, and no quantitative inferences about conformational populations therefore should be made.

Figure 5 shows the variation in the integrated d^+ and d^- peak intensities with the silanization temperature. The plots clearly demonstrate low-temperature plateaus at constant high values of the intensities followed by regimes of monotonically decreasing values, each with a characteristic onset temperature (calculated as before), denoted as T_{cd^+} and T_{cd^-}, observed to be 28 ± 3 and 33 ± 4 °C. Analysis of the structural changes from intensity variations is not straightforward since the spectral intensity will be a function of the coverage (the number of oscillators), the chain orientation (relative orientation of the transition dipole moments of each oscillator and the electric field of the probing light), and the chain conformations[57] (intrinsic structure dependence of the magnitude of the transition dipole moments for each oscillator). For partial coverage films obtained above $T_{cd^\pm}$, the decreasing intensities with increasing temperature thus cannot be assumed to reflect solely the drop in the surface coverage which was determined independently from the ellipsometric data (see previous section).

The changes in the line widths of the d^+ and d^- mode peaks with the preparation temperature are clearly evident in the spectra shown in Figure 3. However, accurate measurements of line widths were prohibitively difficult due to both the overlapping contributions of variable Fermi resonance modes[31,51c] and the insufficient signal-to-noise levels in our spectra. Therefore, critical temperature values were not deduced from these data. Above T_c (a generic value of critical preparation temperature is implied), the line widths increase and become more asymmetric as the temperature increases. The increasing width is straightforwardly interpreted in terms of formation of looser alkyl chain assemblies which contain higher *gauche* defect populations.[58] However, the spectra appear to offer more information. By extensive comparison of the observed peak envelope shapes with those obtained from both crystalline solid and disordered liquid spectra of alkyl chain compounds, it is clear that the observed spectra of the films prepared above T_c do not conform to those of either pure crystalline[51] or pure liquid states.[52] The latter pure phases generally have their spectral intensities distributed around ~2917 or ~2926 cm^{-1}, respectively, whereas the above-T_c film spectra peaks show intensity spread across both regions, especially in the form of sustained intensity at the low-frequency side (d^+ side) and broad tails sloping into the high-frequency edge of the envelope (d^- side). These features would be consistent with the presence of both conformationally ordered and disordered alkyl chains. Further, careful examination of the observed spectra of films prepared above T_c shows that for several preparations, specifically those at 45, 50, and 53 °C, a shoulder on the low-frequency side of the d^- mode absorption envelope is present at ~2919 cm^{-1}, an observation which is consistent with the presence of conformationally ordered phase. The most convincing support for this coexistence is provided in Figure 6, which shows the observed spectrum of a below-T_c film, a simulated spectrum of a hypothetical isotropic monolayer of pure liquid OTS, a simulated solid/liquid mixture spectrum, and finally the actual spectrum observed for a film prepared at 40 °C. The simulation of the

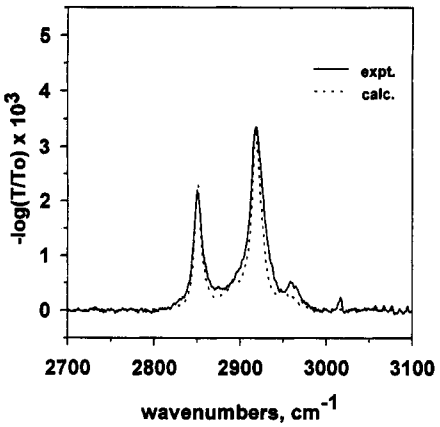

Figure 7. Comparison of an experimental spectrum of an OTS monolayer prepared at 20 °C with a calculated spectrum obtained for a close-packed, crystalline-like assembly of extended *all-trans* octadecylsiloxy molecules with an average chain tilt of 11° from the surface normal.

isotropic liquid film spectrum was carried out using methods described elsewhere,[31] and the values of the required optical function spectra were obtained from measurements on pure OTS liquid in an independent study.[59] The solid–liquid mixture spectrum was obtained by a straightforward linear combination of the independent spectra using a weighting of 75% solid and 25% liquid and appears as the dashed curve in Figure 6. Examination of the spectra in this figure shows that only the simulated mixture spectrum comes close to matching the line shape of the 40 °C film spectrum.[60] This observation strongly suggests that domains of highly conformationally ordered chains coexist with domains of conformationally disordered chains in the above-T_c films. Langmuir films of fatty acids of comparable chain lengths (18–24 carbon chains) at coverages between 22.5 and 35 Å^2 molecule^{-1}, corresponding to those of the above-T_c films (see above), are known to exhibit islandlike morphologies.[61]

Since the spectra of the films prepared at temperatures below T_c infer that the average chain is in an *all-trans* conformation state (possibly as high as 96–99%, as discussed above), it is possible to define a rigid chain axis, and thus a meaningful average tilt angle can be assigned. It has been shown that it is possible to calculate this tilt angle in other self-assembled monolayers from the intensities of the C–H stretching mode absorptions for films of known thickness by using classical electromagnetic theory in conjunction with the frequency spectrum of an optical function tensor for the film material.[31] As part of a larger study involving a series of different substrates, the tilt angles of the present samples have been calculated. The details of the calculation methods will not be presented here as they will be reported elsewhere.[62] The results of simulations for a series of the low-temperature preparation films with an assigned thickness value of (0.93 × 26.2) = 24.4 Å (see Figure 2) yield an average tilt angle value of 11 ± 1°. If the film thicknesses at 86% coverage values were used (22.5 Å), the calculated tilt angle values increases to ~13 ± 1°. The best-fit simulated spectrum for an 11° chain tilt is given in Figure 7 together with a selected companion experimental spectrum for an OTS monolayer prepared at 20 °C.

The above tilt angle can be utilized to calculate the spaces between chains since tilting the chains at constant packing density displaces the chains laterally and increases the area occupied per chain. Using a simple geometric model of a film of contiguous, tilted rods, a chain tilt of θ would correspond to an occupied fraction of the total substrate surface of cos θ and tilt angles in the range of 11–13° would correspond to local chain packing equivalent to coverages of 97.4–98.2%. Note that these values are substantially higher than the ellipsometric estimates of total surface coverage (~86–93%) given in the previous section. As a test of the validity of the high local coverages implied by the tilt angles, the thermal disordering of the films was followed by TIRS with the presumption that the extent of conformational

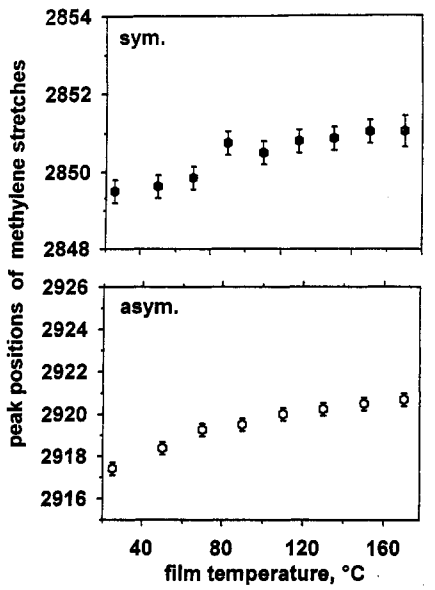

Figure 8. Frequency positions (in cm^{-1}) of d$^+$ and d$^-$ mode peaks observed for an OTS monolayers prepared at 20 °C as a function of the sample temperature during the infrared measurement.

disordering will be strongly limited by the amount of void space which can be made available in the film for chain expansion, and accordingly these high-coverage values effectively immobilize the methylene segments. In bulk crystals, free volume is generated by a three-dimensional expansion of the crystal. However, in the present case of chains pinned at specific sites of a rigid siloxy lattice with invariant position, new volume can be generated only by decreasing chain tilt (at fixed coverage) which opens up space between the chains. If the chains in the above tilted-rod model were kept rigidly pinned to the surface at constant coverage and swung into a vertical orientation ($\theta = 0$), the fractional free volume created within the film would be $\sim(1 - \cos\theta)/\cos\theta$, which for tilt angles of 11–13° correspond to ~2% expansion. Figure 8 shows the temperature-induced changes in peak positions of d$^+$ and d$^-$ modes for an OTS monolayer prepared at 20 °C. The data clearly reveal a very gradual shift in the peak positions toward higher values as the sample temperature is raised, a shift consistent with the expected increasing *gauche* content in the film upon heating. However, the magnitude of the peak frequency shifts with temperature change is remarkably small in comparison with the results of similar studies in bulk *n*-alkanes[63] and other monolayer alkyl chain assemblies of comparably high organization.[64] For example, for *n*-alkanethiolate monolayers on Au(111) surfaces, the d$^+$ and d$^-$ peak positions shift from 2850 and 2918 cm^{-1} at room temperature to 2854 and 2926 cm^{-1} at 160 °C, respectively,[2d] whereas in the present films the corresponding peak shifts over the same temperature range are only 2 and 3 cm^{-1}, respectively.

These observations imply that significantly less free volume is available for chain expansion upon disordering in the case of OTS films compared to alkanethiolates on gold. Using reported values of $\theta \sim 28°$ [65] for the latter film, the tilted rod model shows that the film volume can increase up to ~13% by placing the chains vertical, in contrast to the ~2% value of maximum expansion calculated for OTS films. Thus, the thermal disordering TIRS data support the picture of very high coverages (~98%) with near-vertical tilt angles (11–13°) for the OTS films prepared below T_c.

4. Discussion

4.1. The Existence of a Unique Critical Temperature. The central finding in this study is the common value observed for the six different transition temperatures discussed above: T_{cw}, T_{ce}, T_{cd^+}, T_{cd^-}, T_{cld^+}, and T_{cld^-}. The values range from 23 to 34 °C with an average of ~28 ± 4 °C. Since these T_c's are each derived

from different measures of the film structure, including surface energy, coverage, and conformational ordering, the implication of the unique correspondence of the values is that the chain organization during self-assembly of the OTS monolayer is profoundly affected by solution temperature variations in the vicinity of 28 °C, and thus T_c would appear to be related to an intrinsic behavior of the alkyl chain assembly. This finding provides direct support for a microscopic, structural basis of the previously observed critical preparation temperature, above which film wetting properties deteriorate.[10c,d]

4.2. Strucutres $<T_c$. *4.2.1. Structural Characterization.* The results of the present study show that below T_c, highly oleophobic, dense monolayers with reproducible structural characteristics can be prepared. The γ_c value of these films is extremely low, 20.5 mN m^{-1}, and is in quantitative agreement with the results of the earlier study[10c] which maintained that the surface of these films approaches an ideal, low free energy, pure methyl surface. Further, the almost complete lack of contact angle hysteresis which is observed in all our samples, when interpreted in the framework of current wetting theory,[47] shows that any heterogeneity in the surface distribution of different wettability features, such as voids and discrete film phases, must be of a size scale of ~100 nm or less.

The ellipsometry data give total surface coverages estimated to be in the range 86–93 (±4)% of a monolayer of chains assembled vertically with the density of crystalline polyethylene. Using a packing density of 5.42 chains nm^{-2} for crystalline polyethylene, this coverage range corresponds to a range of surface densities of 4.2–5.2 chains nm^{-2} or molecular areas of 19.8 (±0.7)–21.5 nm^2 chain^{-1}, a range which overlaps with values concluded from XRR[16] and GIXD[17] studies. However, since the ellipsometry data provide average values over large areas, they cannot be used to distinguish whether the chains in the observed films are partially collapsed with a uniform density or arranged heterogeneously in islands.

Infrared vibrational spectroscopy addresses this above issue and shows that the alkyl chains in this dense monolayer exhibit a high fraction of conformations in the *all-trans* extended state with estimated values of 96–99%. The comparison of the observed peak frequencies of the d^+ and d^- modes, 2848.8 ± 0.2 and 2916.8 ± 0.2 cm^{-1}, with the higher values of 2850–51 and 2918–20 cm^{-1} previously reported[11a,14e,19,66] for purported high-quality OTS films suggests slightly higher conformational order in the present films, an indication of an approach to a limiting structure of crystalline-like packing between chains. On the basis of similar infrared spectroscopic data, Buontempo et al.[53] have inferred that heterogeneous, island structures form in Langmuir films. Our observed peak frequencies are consistent with this type of structure, and further analysis as given below supports this conclusion.

The TIRS data show that the average chain in our OTS monolayers prepared below T_c is tilted in a range of 11–13°, in contrast to the 10–18° average tilt derived by Ulman and coworkers[14e] for films of comparable γ_c to ours. Further, on the basis of a simple geometric model, the low tilt angles indicate that in the local vicinity of the chains the coverages are ~98%, and thus only as little as ~2% free volume could be accessed by reorientation of the chains which leaves little space available for the appearance of *gauche* defects. The validity of this high, local coverage is supported by the resistance of these monolayers toward thermal disordering as observed by temperature-dependent TIRS spectra which show (Figure 6) that the $d^\pm$ peak frequencies are nearly temperature invariant. In fact, the spectra show (spectra not shown) that while the films begin to incorporate *gauche* conformers slowly upon heating, this disorder occurs primarily at the chain ends (*t–g* defects) and is relatively minor even at a temperature as high as 160 °C. In an earlier report, Sagiv et al.[11a] characterized the infrared spectral changes during heating of an OTS film prepared on an oxided aluminum substrate. While their spectra show the same qualitative behavior as those in Figure 8, the rate of spectral peak shifting with temperature is significantly greater. We note that their reported initial values of the $d^\pm$ are ~2 cm^{-1} higher than ours, a fact which would indicate a substantially higher *gauche* population, consistent only with a lower film density and thus more free volume accessible to allow more thermal disordering.

In the interpretation of these data in terms of specific monolayer structures, two extreme cases can be considered: (1) homogeneous films, for which a narrow distribution of chain structures are uniformly distributed across the surface, and (2) heterogeneous films, for which domains of ordered, close-packed molecules coexist with disordered molecules along the line boundaries between the domains.

Combining the above picture of densely-packed (local coverage of ~98%), 96–99% *trans* conformation chains oriented nearly vertical to the surface, as inferred from the TIRS data, and the picture of high but incomplete average coverages (~86–93%) inferred from ellipsometry leads to the conclusion that the OTS films prepared below T_c must consist of a heterogeneous structure dominated by islands of highly organized chains. In this picture the missing chain regions would constitute line defects. The wetting hysteresis data require that these islands be on a size scale of less than ~100 nm. Further, the total apolar character of the surface wetting response indicates effective screening of the SiO_2 substrate and suggests molecular-scale dimensions for the island boundary regions (see section 4.2.2). Indeed, small-scale line defects have been observed in recent atomic force microscopy studies of OTS monolayers on SiO_2 surfaces[18a] and hydrated mica.[18b] Finally, such heterogeneous structures are quite consistent with the 45–60-Å in-plane translational correlation lengths derived from recent GIXD measurements on these monolayers.[17]

The above structure of near-vertically-tilted chains packed at high densities imposes a narrow range of structural constraints on the underlying cross-linked siloxy network in the monolayers prepared below T_c. Ulman[5] has addressed this issue and shown that a chair conformation of a siloxy trimer (and even tetramer) species with an Si–O bond distance of 1.63 Å and Si–O–Si and O–Si–O bond angles of 130° and 108.7°, respectively, would create ~4.25–4.35-Å spacing between nearest-neighbor Si atoms, a distance appropriate for chains attached in the axial positions to be tilted at near-vertical angles (≤15°) to the chair plane and packed at near-minimal distances. In fact, it appears from a variety of data[67] that in amorphous SiO_2 structures the Si–O bond distances and the Si–O–Si bond angles can vary over ranges of ~1.61–1.72 Å and 86–152°, leading to nearest-neighbor Si–Si distances over a range of values from 4.25 to 5.0 Å, consistent with the above dense-packed chain structures. Support for these trimer and tetramer siloxy structures can be obtained from infrared reflection spectroscopy measurements of OTS films prepared on gold substrates.[68]

All of the above structural characterization results and literature comparisons underscore the point that the use of the present method of temperature control to prepare limiting-structure films can provide samples which will be precisely reproducible on a lab-to-lab basis and appear to reach a near-limiting structure.

4.2.2. Analysis of Surface Wetting Properties. As all the cumulated evidence in the present study suggests, the below-T_c films appear to represent a limiting structure for OTS monolayers. This structure offers the opportunity to analyze our wetting data for what could be extremely close to the limiting value of the solid–vapor surface tension, γ_{SV}, of a pure methyl character surface. While a number of methods are available for this, we have used two commonly used approaches at the opposite ends of the range of models of wetting behavior: (1) the recent Lifshitz–van der Waals (LW) approach[69] based on a microscopic description of intermolecular forces in which the equilibirum contact angles of a given liquid on a surface results from a sum of solid/liquid interfacial contributions from polar donor–acceptor (acid–base) interactions and apolar Lifshitz–van der Waals type interactions;[70] (2) the Li–Neumann (LN) equation based on a

macroscopic thermodynamic approach.[71,72] This approach has been based on a thermodynamic argument[72c] that a nonhomogeneous interfacial region of finite thickness in real two-component solid–liquid–vapor systems can be replaced by a two-dimensional Gibb's dividing surface when at thermodynamic equilibrium. Li and Neumann[72] have suggested that, by appropriately choosing the position of this dividing surface, a functional relationship exists between the three surface tension terms, *viz.*, $\gamma_{sl} = f(\gamma_s,\gamma_l)$ where γ_{sl}, γ_s, and γ_l are the solid–liquid, solid–vapor, and liquid–vapor surface tensions, respectively. They have derived an exact mathematical form of the functionality by an empirical fitting process applied to a large variety of contact angle data on low-energy polymeric surfaces.[72]

A useful form of the LW approach is embodied in the equation derived by van Oss, Chaudhury, and Good[69,70] (OCG):

$$(1 + \cos\theta)\gamma_l = 2(\sqrt{\gamma_s^{LW}\gamma_l^{LW}} + \sqrt{\gamma_s^{AB}\gamma_l^{AB}})$$

In this equation, the solid–vapor and liquid–vapor interfacial tensions are designated by γ_s and γ_l, respectively, and the superscripts LW and AB designate the Lifshits–van der Waals long-range and Lewis acid–base short-range interactions, respectively. Using hexadecane, a completely apolar liquid, sets the γ^{AB} terms to zero. The observed value of $\theta = 45 \pm 1°$ together with the known liquid–vapor interfacial tension value[72d] of 27.7 mN m^{-1} leads to $\gamma_s^{LW} = 20.2 \pm 0.01$ mN m^{-1}, a value within 1.5% of our measured value of the Zisman critical surface tension, γ_c (20.5, see above). Next, using the contact angle data from water, a highly polar liquid with known values of 21.8, 51.0, and 72.8 mN m^{-1} for γ_l^{LW}, γ_l^{AB}, and γ_l, respectively,[72d] γ_s^{LW} can be calculated. The above data, together with the observed contact angle of $\theta = 114 \pm 2°$ and the value of γ_s^{LW} derived above, results in a value of the acid–base free energy component for the film surface of $\gamma_s^{AB} = 0.00766 \pm 0.0002$ mN m^{-1}. This extremely low value gives an accurate indication of the almost total absence of short-range, chemical interactions (electron-donor electron-acceptor type) available at the CH_3 surface.

The LN approach is expressed in the following equation:

$$\cos\theta = \frac{(0.015\gamma_s - 2.0)\sqrt{\gamma_l\gamma_s} + \gamma_l}{\gamma_l(0.015\sqrt{\gamma_l\gamma_s} - 1)}$$

Using water and hexadecane as the wetting liquids, γ_l = 72.8 and 22.7 mN m^{-1}, respectively, results in γ_s = 22.9 and 22.7 mN m^{-1}. This value is higher by approximately 10% than the value derived above from the OCG equation, suggesting that while the macroscopic approach qualitatively delineates the surface free energy values fairly well, the actual values are better derived from the microscopic description embedded in the OCG equation.

The above results show that, for the limiting methyl surface of our OTS films, the surface free energy γ_{SV} is identical to the Zisman[28] critical surface tension γ_c within experimental error and that the surface is almost perfectly apolar, exhibiting only long-range van der Waals interactions. This observation indicates that the polar, hydrated SiO_2 substrate is completely screened (within experimental sensitivity) from wetting interactions in spite of a heterogeneous OTS film with ~10% uncovered SiO_2 surface. One could reconcile this apparent contradiction if the islands were sufficiently close to allow the outer chains to adopt some small, but sufficient, degree of conformational disorder to fill the spaces, essentially line defects, between the islands. Setting the width of these line defects to ~4.5 Å, the diameter of an *all-trans* chain, and setting the average total surface coverage of these chains to an intermediate value of ~90%, a highly simplistic picture of uniformly-sized, close-packed (implying square or hexagonal shape), crystalline (~5.4 chains nm^{-2}) islands would require an island width of ~50 Å. Such small scale features would be consistent with the observed low values of the wetting hysteresis. It is apparent that all the accumulated evidence from various structural characterizations, including literature reports, as discussed above (section 4.2.1), and the present observations suggests dimensions of ~10 nm associated with the island features in the heterogeneous picture of these films.

4.3. Structures $> T_c$. The results of the present study show that as the preparation temperature increases above T_c the films exhibit decreasing coverages, increasing average conformational disorder, and increasing surface free energy. At 60 °C, the highest preparation temperature used in the present study, the film coverage determined by ellipsometry is lower by 20–25% than that obtained for the films prepared below T_c (see Figure 2). The infrared vibrational spectra of these high-temperature films (see Figure 4) show d^+ and d^- mode peaks at 2852 and 2923 cm^{-1}, respectively, values which approach those associated with highly conformationally disordered chain assemblies; for example, liquid *n*-alkanes show corresponding peaks at 2854–2857 and 2926–2928 cm^{-1}.[52] As a reflection of these disordered structures, the surface free energy (critical surface tension) of the highest temperature preparation films show a value of 22.5 ± 0.2 mN m^{-1}, a value considerably larger than the value of 20.5 mN m^{-1} for the below-T_c films. It should be noted, however, that this value is still far below the value of 31 mN m^{-1} reported for a pure CH_2 surface, such as encountered in polyethylene.[43]

All of the above observations of these films are consistent with the presence of both methylene and methyl groups at the film surface. Specifically, a picture of a structure emerges in which a significant fraction of *gauche* conformers is present at incomplete coverages, a situation which requires the folding of a fraction of the alkyl chains in order to expose CH_2 groups at the air surface.

As with the below-T_c films, two limiting types of film structures can be considered: (1) a homogeneous distribution of partially disordered chains with similar fractions of *gauche* defects or (2) a heterogeneous distribution in which there is a coexistence of regions of ordered and disordered phases. The line shape analyses of the infrared spectra yield strong evidence for the simultaneous presence of both conformationally ordered and disordered claims in our $> T_c$ films. Since it is difficult to imagine any realistic film structure in which isolated *all-trans* extended chains could be found embedded within disordered regions, one can assume that the conformationally ordered species are clustered in domains. The pervasive observation of extremely low hysteresis in our wetting measurements can be interpreted within the framework of current wetting theories[47] to mean that the size of these domains of different wetting character cannot be much greater than ~0.1 μm. The above conclusions thus allow a picture of the films prepared above T_c to consist of a heterogeneous distribution of coexisting microdomains of ordered *all-trans* extended chains and conformationally disordered chains.

4.4. Formation Mechanism. *4.4.1. The Langmuir Film Analogy.* A comprehensive mechanism has been proposed by Brzoska and Rondelez[10d,22] to explain the effects of preparation temperature on the degree of organization in self-assembled *n*-alkylsiloxane films on prehydrated substrates. This mechanism is based on the intermediate presence of an ultrathin interfacial water film upon which mobile, monomeric alkylhydroxysilane species assemble into a Langmuir-like monolayer film which eventually cross-links. This water layer serves several purposes. First, it provides a contributing source of water for hydrolysis of the trichlorosilyl headgroup into a trihydroxysilyl group. Second, it provides a fluid interface upon which the adsorbed molecules can laterally diffuse by Brownian motion to form condensed monolayer phases, a process closely analogous to the formation of condensed Langmuir surfactant phases at the air/bulk water interface.[73] Lastly, it provides an intervening layer between the SiO_2 substrate and the adsorbate which minimizes formation of adsorbate/substrate SiOSi bonds during the film cross-linking step and thus promotes formation of a substrate-decoupled film structure. All data presented in this study can be rationalized within the framework of such a mechanism as will now be developed.

4.4.2. Interfacial Water Layer. Because an adsorbed water film plays such a crucial role in the above mechanism, it is useful to establish what is known about such films on SiO_2 with regard to their presence, stability, and ability to support the adsorbed surfactant overlayers as required by this mechanism. First of all, it has been proposed by Silberzan et al.[10b] and later established by Tripp and Hair[66] that a preadsorbed film of water is required for formation of uniform OTS monolayers on SiO_2. In this regard, it is well-known[74] that the surfaces of clean SiO_2 readily hydrate at ambient temperatures to form uniformly adsorbed water films of at least ~ 1, and up to several, monolayers with the exact value dependent upon the ambient relative humidity. For example, Scott and Traiman[32b] have reported that at 50% relative humidity 3 monolayers of water is adsorbed on a clean silica surface. Upon heating a hydrated SiO_2 sample to ~ 100 °C, the conditions used in the present experiments, weakly bound water is desorbed[19,74] to leave a tenaciously bound film of ~ 1–2 monolayers. However, this residual water is not removed until additional heating to between 170 and 400 °C, and since this desorption is a highly reversible process, efficient removal requires application of high vacuum.[74] Finally, above 400 °C irreversible desorption of the remaining water layer begins to occur.[75] From this evidence, it is clear that the prewetted SiO_2 substrates in the present experiments are covered with an ultrathin film of water, at least ~ 1–2 monolayers thick, prior to immersion in the hexadecane reaction medium. Upon immersion, because of the extremely strong affinity for the substrate, little of this adsorbed water is expected to leave the substrate surface. In support of this, Angst and Simmons[19] have reported infrared spectra of freshly made films of OTS on prehydrated, thermally grown 150–180-Å SiO_2/Si substrates which show the presence of bound water. Second, adsorbed water layers, even thinner than 1 nm, have been shown by Merkel and co-workers[76] to support mobile lipid-monolayer phases whose structures are closely analogous to those of their corresponding Langmuir films. Further, a quantitative correspondence[79] with Langmuir films of lipid bilayers is observed for the phase transition behavior of the hydrated substrate-supported bilayers. This work establishes the existence of a strong parallel between the phase diagrams pertaining to adsorption on bulk water (Langmuir phases) and adsorbed water. However, because of significant differences in the detailed structures and physical properties of the surface of bulk water and that of molecularly thin films of adsorbed water on SiO_2 it is not expected that the associated phase diagrams and phase structures of the surfactant monolayer phases will be identical.[77–79] Since the hydrolyzed OTS molecule $C_{18}H_{37}Si(OH)_3$ is strongly amphiphilic, it is clear that Langmuir-like surfactant phases of the latter should analogously form on adsorbed water films and remain mobile until cross-linked into a siloxy network. In fact, recent experiments[80] show the existence of highly organized, Langmuir films of octadecylsiloxanes at the bulk water surface with sufficient molecular mobilities to show reversible phase transitions in the force–area isotherms.

4.4.3. Temperature-Dependent Phase Behavior of Monomeric Alkylsiloxane Species. The section develops the thermodynamic aspects of the OTS self-assembly mechanism in terms of the analogous *equilibrium* aspects of Langmuir surfactant phases. In a given OTS preparation the following variables remain fixed: (1) film temperature, T, (2) the surface area of the water film forming the adsorbing substrate, and (3) the concentration of silane species in the reactive hexadecane solution, provided that the adsorbed amount is negligible compared to the overall number of solute molecules. Conversely, the following variables adjust according to the course of preparation: (1) the film surface pressure, Π, and (2) the substrate coverage, usefully defined as the alternative quantity, average area per molecule, A_m. Since the system is open in terms of mass transport, the values of A_m and Π vary with the adsorption of solute species. If we make the reasonable assumption that adsorption at the water surface is irreversible because of the strongly H-bonding nature of the –Si-

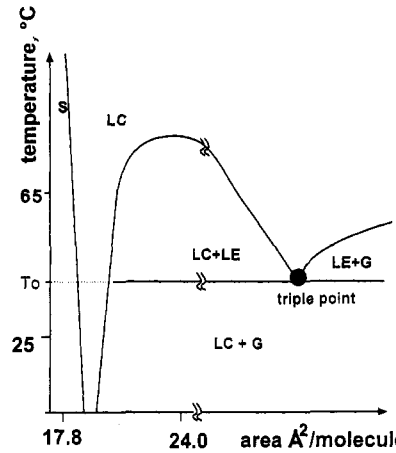

Figure 9. A schematic of a generalized temperature–area per molecule (T–A_m) phase diagram of Langmuir monolayers of fatty acids at an air–water interface. The standard nomenclature for phase descriptions is used: LC, liquid condensed; LE, liquid expanded; G, gas; S, solid. The triple point temperature is represented as T_0.

$(OH)_3$ headgroup and the low solubility in hexadecane, the final value of Π cannot be thermodynamic. Rather, it is set by the solution concentration of adsorbing species and the kinetic barriers of transport of these species through a high-coverage film onto the water surface; clearly, these barriers will scale in some way with coverage. Now consider the generalized T–A_m phase diagram for single alkyl chain surfactant Langmuir monolayers at constant surface pressure, shown in Figure 9. Discussions of such diagrams can be found elsewhere.[24,61a] In this generalized figure, specific values of T and A_m have been added, wherever possible, to correspond to specific phase regions as estimated from known reported values of analogous alkyl surfactant films. Most notable is the existence of several phases, gas (G), liquid expanded (LE), liquid condensed (LC), and solid (S), whose appearance depends upon T and A_m. Further, the possibility exists of extensive coexistence regions between two of these phases. Below the triple point temperature, T_0, G can coexist with a condensed phase whereas above T_0 there is successively a coexistence between G and LE phases at low surface densities, followed by a coexistence between LE and LC phases at higher surface densities. At T_0, G, LE, and LC can coexist. Values of T_0 in the range 38.1–44.5 °C have been reported for octadecanoic acid at the air–water interface.[81]

We explore the above phase diagram with the idea of mapping the behavior of the proposed intermediate octadecylhydroxysilane Langmuir films. The TIRS data for OTS films prepared below T_c (~ 28 °C) show that the structures of the alkyl phase are consistent with an LC phase. On this basis, the self-assembling OTS system obviously allows a continuous adsorption of solute species to form a dilute G phase which condenses to form a highly dense phase. The simplest assumption is that this temperature range is below T_0 and that, as adsorption proceeds, LC domains are progressively formed in the presence of a continuous G phase. This latter phase is very dilute and offers little barrier to further adsorption. Accordingly, the condensed domains grow until the whole surface has reached some maximally dense state. In contrast, for the OTS films prepared at temperatures higher than $T_c \sim 28$ °C, which we now define as an approximation to the triple point temperature of an analogous equilibrium monolayer, is exceeded, and the adsorption initially proceeds from the G phase into the LE phase, much by the same process as above. However, as the homogeneous liquid phase is expanded, further growth involves the formation of LC domains in a continuous LE background. This latter phase creates a considerably larger barrier to adsorption than a G phase, since it is approximately 30 times more dense. From our experimental ellipsometry data we obtain a maximum value of $A_m \sim 25$ Å^2 molecule^{-1} for the films prepared at the highest temperature. This value places the film near the end of the LE–LC coexistence region but certainly

not into a homogeneous phase. This is consistent with the indication of a heterogeneous structure from our TIRS data. It thus appears that these above-T_c films have not reached their thermodynamic equilibrium state. This is supported by the fact that extended reaction times (up to 1 day) results in additional growth to an asymptotic limit, but one which is still below the coverage obtained in far shorter reaction times below T_c. In order to explain this behavior, we propose that in the high-temperature regime the thermodynamics of the intermediate Langmuir films control the structure of the major fraction of the film in the initial formation stages while the final fraction is controlled by the coupled kinetics of growth and cross-linking.

4.4.4. Growth of the Octadecylsiloxane Monolayer. In order to rationalize the hypothesis made in the preceding paragraph, it is necessary to trace the kinetics of film formation. For convenience, selected contributing steps are given below.

$$RSiX_3(soln) \rightleftharpoons RSi(OH)_3(G) \quad (1)$$

$$RSi(OH)_3(G) \rightleftharpoons RSi(OH)_3(S) \quad (2)$$

$$RSi(OH)_3(G) \rightleftharpoons RSi(OH)_3(LC) \quad (3)$$

$$RSiX_3(soln) + [RSi(OH)_3(S,LC)]_n \rightleftharpoons [RSi(OH)_3(S,LC)]_{n+1} \quad (4)$$

$$2RSi(OH)_3(film) \rightleftharpoons R[(OH)_2]Si\text{–}O\text{–}Si(OH)_2R + H_2O \quad (5)$$

$$RSi(OH)_3(G) \rightleftharpoons RSi(OH)_3(LE) \quad (6)$$

$$RSiX_3(soln) + [RSi(OH)_3(LE)]_n \rightleftharpoons [RSi(OH)_3(LE)]_{n+1} \quad (7)$$

$$RSi(OH)_3(LE) \rightleftharpoons RSi(OH)_3(LC) \quad (8)$$

Below T_0 the following sequence of steps is proposed. Initially, a solution alkylsilane species, either the trichlorosilane or some hydrolyzed derivative,[82] adsorbs onto the substrate water film with the eventual appearance of an alkyltrihydroxysilane in a G phase (step 1). As the coverage grows and Π increases, LC phases appear (steps 2 and 3). As the coverage reaches very high values little free surface remains, and presumably the limit would be close-packed islands separated by line defects of a width approaching the diameter of a single chain. At this point adsorption of a solute molecule at the free water surface effectively becomes blocked, and further adsorption must occur via penetration into some type of defect (dynamic or static) region (step 4) in the dense phases. Finally, at some late stage in the film growth, cross-linking occurs as represented by step 5, depicted as a simple bimolecular condensation reaction. Since the final film structures so closely resemble the compact LC phases of model surfactant systems, it is apparent that step 5 is slow compared to the preceding steps and that the cross-linking must occur compliantly, *viz*, with minimal introduction of strain in the film lattice. In view of the range of possible Si–O bond distances and Si–O–Si bond angles which are compatible with the structures required for a dense-packed hydrocarbon phase (see section 4.2.1), such compliance seems quite reasonable, especially if the degree of cross-linking is light. This series of steps also infers a film formation mechanism involving initial growth at the edges of islands formed at a number of dispersed nucleation sites. Such a growth mechanism will lead to a heterogeneous, island structure with quite narrow boundary regions, a picture completely consistent with the one discussed earlier (sections 4.2.1 and 4.2.2).

Above T_0 the major thermodynamic factor is the appearance of an LE phase. This leads to the entrance of steps 6 and 8. However, the significant issues center on two kinetic factors proposed to inhibit the approach to establishment of equilibrium phases. Specifically, as temperature is increased, it is proposed that the adsorption rate will *decelerate* and the cross-linking rate *accelerate*, relative to the corresponding rates for identical, moderate- to high-coverage films forming below T_c. First of all, as the triple point temperature T_0 is exceeded, the equilibrium phase at higher coverages shifts from LC to LE + LC coexistent phases and adsorption occurs via steps 1, 3, and 5. One important distinction between films above and below T_0 is that, for equal values of molecular surface coverage, the low-T films of G + (LC or S) phases should exhibit a larger fraction of actual open water surface than for the high-T films with the G + (LC + LE) phases because the replacement of LC (or S) phases with LE results in thinner films but with more spread out alkyl tails, effectively covering more water surface. This effect should result in some diminution in the rate of adsorption in the above-T_0 regime by forcing the process from step 1 to the slower steps 4 and 7. The second and critical factor involves the proposal that cross-linking (step 5) accelerates more with increasing T than does film growth. This situation appears reasonable in view of the fact that chemical bonding changes are involved, and these would be expected to have a greater activation energy than surface diffusion and structural relaxation processes. The consequences of early cross-linking should be the "freezing" in of additional defects in the films and an accompanying drop in surface density because of the poor chain packing, consistent with the observed effects. Further, the observation of continued slow, asymptotic growth at extended times for only the higher temperatures can be rationalized in terms of the early rigidification of the film in a dominantly LE phase structure, populated by frozen, nonequilibrium defects. Incorporation of a new solute species into the interior of a film domain would become difficult because of the presence of covalent bonding between siloxy groups in the existing film. This leaves population of the voids as the only growth channel left, a process which would presumably occur slowly by a direct adsorption from solution into the voids. Further, some defects would remain and the ultimate films should exhibit lower densities than equilibrium films, a prediction in complete accord with our observations.

5. Conclusions

A major finding of this study is the observation that deposition of OTS films with reproducible molecular structures can be accomplished by control of the solution temperature below a critical value of $T_c \sim 28 \pm 5$ °C. Since this temperature is within the range of typical ambient variations, this finding provides one basis to explain lab-to-lab irreproducibility of film preparations. The variation of structures for films prepared at different temperatures can be rationalized through an analogy between the critical temperature and the triple point temperature for C_{18} Langmuir monolayers at the air–water interface, typically observed in the range 33–44 °C. This analogy is supported by the close correspondence of these two temperatures and by the requirement of prehydration of the substrate surfaces for high-quality film formation.[19]

Acknowledgment. The authors thank J. B. Brzoska for his cooperation in performing the initial silanization experiments. We also thank Professor H. Möhwald for valuable suggestions during the writing of this manuscript. Support from the National Science Foundation (DMR 900-1270, D.A. and A.P.), CNRS (I.A. and F.R.), Elf-Atochem (I.A.), and Elf-Aquitaine (F.R.) is gratefully acknowledged.

References and Notes

(1) (a) Swalen, J. D.; Allara, D. L.; Andrade, J. D.; Chandross, E. A.; Garoff, S.; Israelachvilli, J.; McCarthy, T. J.; Murray, R.; Pease, R. F.; Rabolt, J. F.; Wayne, K. J.; Yu, H. *Langmuir* **1987**, *3*, 932–950. (b) Ulman, A. *Introduction to Ultra-thin Organic Films: From Langmuir Blodgett to Self-Assembly*; Academic: San Diego, CA, 1991.

(2) (a) Silberzan, P.; Leger, L. *Phys. Rev. Lett.* **1991**, *66*, 185–188. (b) Whitesides, G. M.; Laibinis, P. E. *Langmuir* **1990**, *6*, 87–96. (c) Dubois, L. H.; Nuzzo, R. G. *Annu. Rev. Phys. Chem.* **1992**, *43*, 437–463 and references therein.

(3) (a) Chaudhury, M. K.; Whitesides, G. M. *Science* **1992**, *255*, 1230–1232. (b) Israelachvili, J. N. In *Fundamentals of Friction: Macroscopic and Microscopic Processes*; Kluwer Academic: Amsterdam, The Netherlands, 1992; pp 351–385.

(4) (a) Polymeropolous, E. E.; Sagiv, J. *J. Chem. Phys.* **1978**, *69*, 1836–1847. (b) Finklea, H. O.; Robinson, L. R.; Blackburn, A.; Richter, B.; Allara, D.; Bright, T. *Langmuir* **1986**, *2*, 239–244. (c) Sabatini, E.; Rubeinstein, I.; Maoz, R.; Sagiv, J. *J. Electroanal. Chem.* **1987**, *219*, 365–371. (d) Kim, J.-J.; Cotton, T. M.; Uphaus, R. A. *J. Phys. Chem.* **1988**, *92*, 5572–5578. (e) Bard, A. J.; Abruna, H. D.; Chidsey, C. E.; Faulkner, L. R.; Feldberg, S. W.; Itaya, K.; Majda, M.; Melroy, M.; Murray, R. W.; Porter, M. D.; Soriaga, M. P.; White, H. S. *J. Phys. Chem.* **1993**, *97*, 7147–7174 and selected references therein.

(5) Ulman, A. *Adv. Mater.* **1990**, *2*, 573–582 and selected references therein.

(6) (a) Tiberio, R.; Craighead, H. G.; Lercel, M.; Lau, T.; Sheen, C. W.; Allara, D. L. *Appl. Phys. Lett.* **1993**, *62*, 476–478. (b) Lercel, M. J.; Tiberio, R. C.; Chapman, P. F.; Craighead, H. G.; Sheen, C. W.; Parikh, A. N.; Allara, D. L. *J. Vac. Sci. Technol., B* **1993**, *11*, 2823–2828.

(7) (a) Laibinis, P. E.; Hickman, J. J.; Wrighton, M. S.; Whitesides, G. M. *Science* **1991**, *245*, 845–847. (b) Rubinstein, A.; Steinberg, S.; Tar, Y.; Shanzer, A.; Sagiv, J. *Nature (London)* **1988**, *332*, 426–429. (c) Dulcey, C. S.; Georger, J. H.; Krauthamer, V.; Stenger, D. A.; Fare, T. L.; Calvert, J. M. *Science* **1991**, *252*, 551–554. (d) Prime, K. L.; Whitesides, G. M. *Science* **1991**, *252*, 1164–1167. (e) Stenger, D. A.; Georger, J. H.; Dulcey, C. S.; Hickman, J. J.; Rudolph, A. S.; Nielson, T. B.; McCort, S. M.; Calvert, J. M. *J. Am. Chem. Soc.* **1992**, *114*, 8435–8442. (f) Spinke, J.; Liley, M.; Gruder, H.-J.; Angermaier, L.; Knoll, W. *Langmuir* **1993**, *9*, 1821–1825. (g) Ratner, B. D.; Ertel, S. A.; Atre, S. V.; Allara, D. L. *Langmuir*, in press.

(8) Pluedemann, E. P. *Silane Coupling Agents*; Plenum: New York, 1990.

(9) (a) Sagiv, J. *J. Am. Chem. Soc.* **1980**, *102*, 92–98. (b) Netzer, L.; Sagiv, J. *J. Am. Chem. Soc.* **1983**, *105*, 674–676.

(10) (a) Wasserman, S. R.; Tao, Y.-T.; Whitesides, G. M. *Langmuir* **1989**, *5*, 1074–1087. (b) Silberzan, P.; Leger, L.; Aussere, D.; Benattar, J. J. *Langmuir* **1991**, *7*, 1647–1651. (c) Brzoska, J. B.; Shahidzadeh, N.; Rondelez, F. *Nature* **1992**, *360*, 719–721. (d) Brzoska, J. B.; Rondelez, F., submitted to *Langmuir*.

(11) (a) Cohen, S. R.; Naaman, R.; Sagiv, J. *J. Phys. Chem.* **1986**, *90*, 3054–3056. (b) Fontaine, P.; Guguenheim, D.; Deresmes, D.; Vuillame, D.; Garet, M.; Rondelez, F. *Appl. Phys. Lett.* **1993**, *62*, 2256–2258.

(12) (a) Moaz, R.; Sagiv, J. *Langmuir* **1987**, *3*, 1045–1051. (b) *Ibid.* **1987**, *3*, 1034–1044.

(13) (a) Nuzzo, R. G.; Allara, D. L. *J. Am. Chem. Soc.* **1983**, *105*, 4481–4482. (b) Bain, C. D.; Whitesides, G. M. *Angew. Chem., Int. Ed. Engl.* **1989**, *101*, 506–512.

(14) (a) Netzer, L.; Iscovici, R.; Sagiv, J. *Thin Solid Films* **1983**, *100*, 67–76. (b) Maoz, R.; Sagiv, J. *J. Colloid Interface Sci.* **1984**, *100*, 465–496. (c) Gun, J.; Iscovici, R.; Sagiv, J. *J. Colloid Interface Sci.* **1984**, *101*, 201–214. (d) Gun, J.; Sagiv, J. *J. Colloid Interface Sci.* **1986**, *112*, 457–472. (e) Tillman, N.; Ulman, A.; Schildkraut, J. S.; Penner, T. L. *J. Am. Chem. Soc.* **1988**, *111*, 6136–6144.

(15) Guyot-Sionnet, P.; Superfine, R.; Hunt, J. H.; Shen, Y. R. *Chem. Phys. Lett.* **1988**, *144*, 1–5.

(16) Wasserman, S. R.; Whitesides, G. M.; Tidswell, I. M.; Ocko, B. M.; Pershan, P. S.; Axe, J. D. *J. Am. Chem. Soc.* **1989**, *111*, 5852–5861.

(17) Tidswell, I. M.; Rabedeau, T. A.; Pershan, P. S.; Kosowsky, S. D.; Folkers, J. P.; Whitesides, G. M. *J. Chem. Phys.* **1991**, *95*, 2854–2861.

(18) (a) Barrat, A.; Silberzan, P.; Bourdieu, L.; Chatenay, D. *Europhys. Lett.* **1992**, *20*, 633–638. (b) Schwartz, D. K.; Steinberg, S.; Israelachvili, J.; Zasadzinski, J. A. N. *Phys. Rev. Lett.* **1992**, *69*, 3354–3357.

(19) Angst, D. L.; Simmons, G. W. *Langmuir* **1991**, *7*, 2236–2242.

(20) Garoff, S.; Hall, R. B.; Deckman, H. W.; Alvarez, M. S. *Proc. Electroanal. Chem.* **1985**, *112*, 85–94.

(21) (a) Tripp, C. P.; Hair, M. L. *Langmuir* **1992**, *8*, 1120–1126. (b) LeGrange, J. D.; Markham, J. L.; Kurkjian, C. R. *Langmuir* **1993**, *9*, 1749–1754.

(22) Brzoska, J. B. Thèse, Université Paris VI, 1993.

(23) Fully hydrated SiO_2 surfaces contain ~5 silanol groups per nm^2 (Zhuravlev, L. T. *Langmuir* **1987**, *3*, 316–318).

(24) (a) Knobler, C. M.; Desai, R. C. *Annu. Rev. Phys. Chem.* **1992**, *43*, 207–236 and selected references therein. (b) Knobler, C. M. *Adv. Chem. Phys.* **1990**, *77*, 397–449.

(25) Frantz, P.; Granick, S. *Langmuir* **1992**, *8*, 1176–1182.

(26) Vig, J. R. *J. Vac. Sci. Technol., A* **1985**, *3*, 1027–1033.

(27) (a) Allain, C.; Aussere, D.; Rondelez, F. *J. Colloid Interface Sci.* **1985**, *107*, 5–13 and references therein.

(28) Zisman, W. A. *Adv. Chem. Ser.* **1964**, *No. 43*, 1–51.

(29) (a) Azzam, R. M. A.; Bashara, N. M. *Ellipsometry and Polarized Light*; North-Holland: Amsterdam, The Netherlands, 1977, and selected references therein. (b) Aspnes, D. E. In *Optical Properties of Solids: New Developments*; North-Holland: Amsterdam, The Netherlands, 1976; Chapter 15. (c) Yeh, P. *Optical Waves in Layered Media*; Wiley-Interscience: New York, 1988.

(30) Parikh, A. N.; Allara, D. L. In *Spectroscopic Ellipsometry of Heterogeneous Thin Films*; Vedam, K., Ed.; Academic: New York, in press.

(31) Parikh, A. N.; Allara, D. L. *J. Chem. Phys.* **1992**, *96*, 927–945.

(32) (a) Hair, M. L.; Hertl, W. *J. Phys. Chem.* **1969**, *73*, 4269–4276. (b) Scott, R. W.; Traiman, S. *J. Chromatogr.* **1980**, *196*, 193–205.

(33) Carim, A. H.; Dovek, M. M.; Quate, C. F.; Sinclar, R.; Vorst, C. *Science* **1987**, *237*, 630–632.

(34) These errors were estimated through simulations of the ellipsometric measurements using known values of the dielectric functions for each phase together with the range of water, SiO_2, and OTS film thicknesses expected. In these calculations, values of 1.33 + 0*i*, 1.45 + 0*i*, and 3.882 + 0.019*i*, obtained from the literature (*Handbook of Optical Constants of Solids II*; Palik, E. D., Ed.; Academic: Orlando, FL, 1985) were assigned for the refractive indices of H_2O, SiO_2, and Si, respectively. The results of the calculations show that differences between the OTS film thicknesses based on the two models are within 0.25 Å for OTS films of ≤26-Å thickness, an insignificant error in comparison to our experimentally observed sample-to-sample errors of ±1 Å.

(35) Israelachvili, J. N.; Pashley, R. M. *Nature* **1993**, *306*, 249–250.

(36) *Polymer Handbook*; Brandrup, J.; Immergut, E. H., Eds.; John Wiley: New York, 1975; Vol. 13, p V-22.

(37) den Engelsen, D. *Surf. Sci.* **1976**, *56*, 272–280.

(38) It has been shown in ref 37 that the values of $n_\parallel$ and $n_\perp$ for alkyl chains are somewhat dependent upon the nature the terminal group, i.e., X in $CH_3(CH_2)_nX$, because of the contribution of X to the overall volume polarizability. For the two functional groups X = –COOH and (–$COOBa_{1/2}$) with an octadecyl (n = 18) chain, the calculated effects (ref 32) were noted to cause a change of 0.57% in $n_\perp$ and 1.6% in $n_\parallel$. Although such information for siloxy group present in our OTS monolayers was not directly available, we have assumed that the magnitude of the effects on $n_\parallel$ and $n_\perp$ to be of similar size. Our preliminary calculations of film thicknesses suggest that even as high a change as 2% in $n_\parallel$ and $n_\perp$ causes a change of less than 0.5 Å for a 25-Å film on an oxidized, hydrated silicon surface, well below our experimental errors in the ellipsometric measurements. Accordingly, we have ignored the headgroup effects on $n_\parallel$ and $n_\perp$ and used the values reported in ref 37 for $CH_3(CH_2)_nCOOH$.

(39) (a) Allara, D. L.; Nuzzo, R. G. *Langmuir* **1987**, *1*, 52–66. (b) McCrackin, F. L.; Passaglia, E.; Stromberg, R. R.; Steinberg, H. L. *J. Res. Natl. Bur. Stand., Sect. A* **1963**, *67*, 363–377.

(40) If the decrease in surface density were to result in the disordering of the chains, a decrease in the corresponding *volume* density of the film would result, represented in the extreme limit by the type of change which occurs in the melting of *n*-alkanes. This in turn would require the use of a correspondingly lower refractive index value for the calculation of ellipsometric thicknesses. However, the lowest film coverages we observe are ~75%, and the effects of refractive index variation in the 75–100% coverage range are expected to be close to our experimental measurement errors. For example, using an extreme value of 1.43, the approximate value for a completely liquid paraffin, rather than the value of 1.50, leads to an increase in the calculated film thickness of 0.8 Å. It should be noted that the numerical magnitude of these effects are specific to the sample material and structure under consideration, *viz.*, film/SiO_2/Si.

(41) Buontempo, J. T.; Rice, S. A. *J. Chem. Phys.* **1993**, *98*, 5835–5846.

(42) A standard four-parameter logistic function was used to fit a sigmoidal function through the experimental data. (See for example: Agresti, A. *Analysis of Ordinal Categorical Data*; Wiley-Interscience: New York, 1984.)

(43) Fox, H. W.; Zisman, W. A. *J. Colloid Interface Sci.* **1952**, *7*, 428–442.

(44) Recently, there have been efforts to develop theoretical models which incorporate the discrete nature of surface phases at molecular length scales (See, for example: Joanny, J. F.; deGennes, P. G. *Physica (Amsterdam)* **1987**, *147A*, 238–255.)

(45) Good, R. J. *J. Am. Chem. Soc.* **1952**, *74*, 5041. (b) Morra, M.; Occhiello, E.; Garbassi, F. *Adv. Colloid Interface Sci.* **1990**, *32*, 79–116 and references therein. (c) Robbins, M. O.; Joanny, J. F. *Europhys. Lett.* **1987**, *3*, 729–735.

(46) The time scales involved are larger than the measurement time. Surface changes include reorientation of polar surface groups, penetration of the probe liquid, and consequent swelling of the solid surface. See, for example: Andrade, J. D.; Smith, L. M.; Gregonis, D. E. In *Surface and Interface Aspects of Biomedical Polymers*; Andrade, J. D., Ed.; Plenum Press: New York, 1985; Vol. 1, Chapter 7 and selected references therein.

(47) (a) Schwartz, L. W.; Garoff, S. *Langmuir* **1985**, *1*, 219–230. (b) Joanny, J. F.; deGennes, P. G. *J. Chem. Phys.* **1984**, *81*, 552–562.

(48) However, we note that no information was given in the report of Wasserman et al. (ref 10a) with regard to the amount of adsorbed water in either the substrate reference sample (used for determination of substrate pseudooptical constants as cleaned and hydrated uncoated silicon substrates maintained under water prior to measurements) or the final film, so direct comparisons are difficult within perhaps 2 Å or an ~8% coverage spread.

(49) Geil, P. H. *Polymer Single Crystals*; Wiley-Interscience: New York, 1963.

(50) Dubois, L. H.; Nuzzo, R. G.; Allara, D. L. *J. Am. Chem. Soc.* **1990**, *112*, 558–569.

(51) (a) Snyder, R. G.; Schachtschneider, J. H. *Spectrochim. Acta* **1963**, *19*, 85–116. (b) MacPhail, R. A.; Strauss, H. L.; Snyder, R. G.; Elliger, C. A. *J. Phys. Chem.* **1982**, *88*, 334–341. (c) Snyder, R. G.; Hsu, S. L.; Krimm, S. *Spectrochim. Acta, Part A* **1978**, *34*, 395–406. (d) Hill, I. R.; Lewin, I. W. *J. Chem. Phys.* **1979**, *70*, 842–581.

(52) Snyder, R. G.; Strauss, H. L.; Elliger, C. A. *J. Phys. Chem.* **1982**, *86*, 5145–5150.

(53) Buontempo, J. T.; Rice, S. A.; Karaborni, S.; Siepmann, J. I. *Langmuir* **1993**, *9*, 1604–1607.

(54) Karaborani, S. *Langmuir* **1993**, *9*, 1334–1343 and selected references therein.

(55) See, for example: Wolf, S. G.; Deutsch, M.; Landau, E. M.; Lahav, M.; Leiserowitz, L.; Kjaer, K.; Als-Neilsen, J. *Science* **1988**, *242*, 1286.

(56) See, for example: Harris, J. G.; Rice, S. A. *J. Chem. Phys.* **1992**, *96*, 1352–1358.

(57) Snyder, R. G. *Macromolecules* **1990**, *23*, 2081–2087.

(58) (a) Cameron, D. G.; Casal, H. L.; Mantsch, H. H. *Biochemistry* **1980**, *19*, 3665–3672. (b) Wood, K. A.; Snyder, R. G.; Strauss, H. L. *J. Chem. Phys.* **1989**, *91*, 5255–5262.

(59) Parikh, A. N.; Allara, D. L. Manuscript in preparation. [Optical constants of OTS films and liquid are available upon request (D.L.A.).]

(60) It would seem logical that the above type of spectral analysis could be extended to analyze for the proportions of the phase components by the application of curve-fitting procedures, but in our opinion, the lack of quantitative characterization of the intrinsic intensities of the component peaks in the overall peak envelopes of each major spectral feature and the actual complexities of the spectra because of Fermi resonance features (refs 51c and 31) precludes such quantitative analyses.

(61) (a) Knobler, C. M. *Science* **1990**, *249*, 870 and selected references therein. (b) Lin, B.; Shih, M. C.; Bohanon, T. M.; Ice, G. E.; Dutta, P. *Phys. Rev. Lett.* **1990**, *65*, 191–194. (c) Schlossman, M. L.; Schwartz, D. K.; Pershan, P. S.; Kawamoto, E. H.; Kellogg, G. J.; Lee, S. *Phys. Rev. Lett.* **1991**, *66*, 1599–1602.

(62) In brief, the optical function tensor is determined from experimentally obtained spectra of a reference material of acceptably similar structure to the film material but existing in another sample configuration. In this method, the optical tensor matrix element contributions of individual vibrational modes (oscillators) are determined by curve resolution of the reference spectra, and each mode (oscillator) is assigned a transition dipole moment direction. It is these directions which connect the spectral response to the molecular orientation. The reference samples used in the present calculations consisted of a set of several different monofunctional octadecyl compounds. Quantitative mixtures of these reference compounds and KBr were formed into disks, spectra were collected above and below the melting transitions, and consistent correlations between the relative changes in the mode intensities of the $d^{\pm}$ mode features with melting were established. Spectra of bulk liquid-phase samples of hydrolyzed OTS were obtained using a 45° prism cell. These measurements used to set the basis for the correct intensity of the desired optical functions, and consistent intensity relationships between solid- and liquid-phase spectra for the reference compounds were used to correct for structural phase differences in the spectra. The optical functions used here were shown to be self-consistent in the sense that spectra of similar OTS monolayer films taken under different conditions, e.g., reflection spectra at different angles and beam polarizations, were all quantitatively simulated with the identical set of functions, thus demonstrating the uniqueness of the functions. Complete details of these calculations are beyond the scope of the present paper and will be presented elsewhere together with the optical function data (ref 59).

(63) Snyder, R. G.; Maroncelli, M.; Strauss, H. L.; Hallmark, V. M. *J. Phys. Chem.* **1986**, *90*, 5623–5630.

(64) (a) Nuzzo, R. G.; Korenic, E. M.; Dubois, L. H. *J. Chem. Phys.* **1990**, *93*, 767–773. (b) Dubois, L. H.; Zegarski, B. R.; Nuzzo, R. G. *J. Electron Spectrosc. Relat. Phenom.* **1990**, *54/55*, 1143–1152.

(65) (a) Laibinis, P. E.; Whitesides, G. M.; Allara, D. L.; Tao, Y.-T.; Parikh, A. N.; Nuzzo, R. G. *J. Am. Chem. Soc.* **1991**, *113*, 7152–7167. (b) Fenter, P.; Eisenberger, P.; Liang, K. S. *Phys. Rev. Lett.* **1993**, *70*, 2447–2451.

(66) (a) Ulman, A.; Tillman, N. *Langmuir* **1989**, *5*, 1418–1420. (b) Kallury, K. M. R.; Thompson, M.; Tripp, C. P.; Hair, M. L. *Langmuir* **1992**, *8*, 947–954. (c) Pomerantz, M.; Segmuller, A.; Netzer, L.; Sagiv, J. *Thin Solid Films* **1985**, 153–162.

(67) (a) Bunker, B. C.; Haaland, D. M.; Ward, K. J.; Michalske, T. A.; Smith, W. L.; Binkley, J. S.; Melius, C. F.; Balfe, C. A. *Surf. Sci.* **1989**, *210*, 406. (b) Dubois, L. H.; Zegarski, B. R. *J. Phys. Chem.* **1993**, *97*, 1665–1670.

(68) Parikh, A. N.; Liedberg, B.; Atre, S. V.; Ho, M.; Allara, D. L. Submitted for publication.

(69) (a) van Oss, C. J.; Good, R. J.; Chaudhury, M. K. *J. Colloid Interface Sci.* **1986**, *111*, 378–390. (b) van Oss, C. J.; Chaudhury, M. K.; Good, R. J. *Adv. Colloid Interface Sci.* **1987**, *28*, 35–64. (c) van Oss, C. J.; Chaudhury, M. K.; Good, R. J. *Chem. Rev.* **1988**, *88*, 927–941 and selected references therein.

(70) In the LW approach, the division of polar and apolar components is based on a finding by Lifshitz (Dzyoloshinskii, I. E.; Lifshitz, E. M.; Pitaevskii, L. P. *Adv. Phys.* **1961**, *10*, 165–209) that all electrodynamic forces in condensed matter phases (namely, London dispersion, Keesom dipole–dipole, and Debye dipole–induced dipole forces) decay with distance at the same rate and are thereby uniformly additive. In contrast, Lewis acid–base or electron donor–acceptor interactions are chemical in nature, and as such these forces decay much more rapidly with distance. In the approach proposed by van Oss, Chaudhury, and Good, the solid–vapor interfacial tension can be represented as a linear combination of components from the above two interactions, and the contribution from each can be identified from the values of equilibrium contact angles of polar and apolar test liquids of known liquid–vapor surface tensions.

(71) Central to this "equation of state" approach is a thermodynamic argument asserting that the solid–liquid surface tension is only a function of the solid–vapor and liquid–vapor surface tensions, which, in conjunction with Young's equation (Young, T. *Philos. Trans. R. Soc. London* **1805**, *95*, 65), explicitly defines the contact angle. This relationship allows the surface tension of a solid to be determined solely from a contact angle of a liquid of known surface tension, regardless of its contributing interactions. To derive explicit forms of these equations, Li and Neumann resorted to empirical methods of parametrization and evaluated the values by contact angle measurements on a range of low-energy surfaces.

(72) (a) Ward, C. A.; Neumann, A. W. *J. Colloid Interface Sci.* **1974**, *49*, 286–290. (b) Neumann, A. W.; Good, R. J.; Hope, C. J.; Sejpal, M. *J. Colloid Interface Sci.* **1974**, *49*, 291–304. (c) Li, D.; Neumann, A. W. *Adv. Colloid Interface Sci.* **1992**, *39*, 299–345.

(73) Gaines, G. L., Jr. *Insoluble Monolayers at Liquid-Gas Interfaces*; Wiley-Interscience: New York, 1966 and references therein.

(74) See, for example: (a) Hair, M. L. *Infrared Spectroscopy in Surface Chemistry*; Marcel Dekker: New York, 1967. (b) Iler, R. K. *The Chemistry of Silica*; John Wiley: New York, 1979.

(75) (a) Young, G. J. *J. Phys. Chem.* **1958**, *13*, 67. (b) Fripiat, J. J.; Gastuche, M. C.; Brichard, R. *J. Phys. Chem.* **1962**, *66*, 805.

(76) Merkel, R.; Sackman, E.; Evans, E. *J. Phys. Fr.* **1989**, *50*, 1535–1555.

(77) The structures and physical properties (ref 78) of ultrathin water films adsorbed at solid substrates will differ from those of their bulk counterpart through the influences of substrate chemistry, surface roughness, presence of chemical heterogeneities, and specific defects on the substrate surface. In the specific case of the present experiments, the strong hydrogen-bonding character of the SiO_2 substrates causes strong perturbations in both the water structure and the fluidity, as manifested in viscosity and diffusion. It is known for the case of substrate-bound, ultrathin water films that these latter properties are intermediate between those of ice and bulk liquid water (refs 76 and 79). However, the use of high-purity, highly polished (~5-Å surface roughness as compared with an ~3-Å roughness of a bulk water surface [ref 78c]) silicon substrates should minimize the effects of roughness, heterogeneity, and defects. Finally, we point out that van der Waals interactions between the adsorbed surfactant phases and the substrate will also influence the character of the surfactant phase.

(78) (a) Garoff, S.; Sirota, E. B.; Sinha, S. K.; Stanley, H. B. *J. Chem. Phys.* **1989**, *90*, 7505–7515. (b) Aussere, D.; Picard, A. M.; Leger, L. *Phys. Rev. Lett.* **1986**, *57*, 2671–2675. Andelman, D.; Joanny, J. F.; Robbins, M. O. *Europhys. Lett.* **1988**, *7*, 731.

(79) (a) Zarko, V. I.; Tumanov, A. A. *React. Kinet. Catal. Lett.* **1993**, *50* (1/2), 189–192. (b) Israelachvili, J.; McGuiggan, P.; Gee, M.; Homola, A.; Robbins, M.; Thompson, P. *J. Phys.: Condens. Matter* **1990**, *2*, SA89-SA98 and selected references therein.

(80) (a) Sharma, R.; Woods, J. Preprint. (b) Parikh, A. N.; Sharma, R.; Allara, D. L. Manuscript in preparation.

(81) (a) Smith, T. J. *J. Colloid Interface Sci.* **1967**, *23*, 27–35. (b) Asgharian, B.; Cadenhead, D. A. *J. Colloid Interface Sci.* **1990**, *134*, 522–533. (c) Kellner, B. M.; Müller-Landau, F.; Cadenhead, D. A. *J. Colloid Interface Sci.* **1978**, *66*, 597–601.

(82) For completeness, we note that it is possible that the hexadecane solution may contain oligomeric species and/or self-assembled microphases (e.g., inverse micelles or bilayers) of hydrolyzed OTS solute molecules. In general, the exact type of solute species would be a function of the concentration of dissolved water, the specific solvent(s), and the solution temperature. Because of the large variety of possibilities, such solution species are not indicated explicitly in the listed reactions. The presence of oligomeric species has been suggested in the AFM studies of Schwartz et al. (ref 18b) and Ulman (ref 5).